Table 3. Classification of Highly (>3-Fold) Expressed Genes in ASC According to Gene Ontology Terms

Category	% of genes in category	% of genes in list in category	P value
0007067: Mitosis	1.3	11.4	4.43×10^{-24}
0000279: M phase	1.8	12.4	6.87×10^{-22}
0000278: Mitotic cell cycle	2.2	12.7	2.53×10^{-19}
0007049: Cell cycle	7.0	21.1	3.23×10^{-16}
0007059: Chromosome segregation	0.31	4.14	6.51×10^{-12}
0006260: DNA replication	1.3	7.32	9.94×10^{-12}
0007088: Regulation of mitosis	0.34	3.82	3.10×10^{-10}
0000070: Mitotic sister chromatid segregation	0.15	2.86	3.11×10^{-10}
0051301: Cell division	0.79	5.41	3.30×10^{-10}
0006955: Immune response	5.7	14.9	1.15×10^{-9}
0007017: Microtubule-based process	1.6	7.32	1.60×10^{-9}
0007093: Mitotic checkpoint	0.13	2.54	2.01×10^{-9}
0000074: Regulation of progression through cell cycle	4.5	12.7	2.77×10^{-9}
0006259: DNA metabolism	4.8	13.1	5.12×10^{-9}
0006952: Defense response	6.2	15.2	7.53×10^{-9}
0009613: Response to pest, pathogen or parasite	3.5	10.8	8.31×10^{-9}
0000075: Cell cycle checkpoint	0.44	3.82	9.71×10^{-9}
0009607: Response to biotic stimulus	6.6	15.6	1.32×10^{-8}
0043207: Response to external biotic stimulus	3.7	10.8	1.73×10^{-8}
0006950: Response to stress	9.2	19.1	3.41×10^{-8}
0031577: Spindle checkpoint	0.084	1.91	7.56×10^{-8}
0007018: Microtubule-based movement	0.87	4.77	8.72×10^{-8}
0006954: Inflammatory response	1.6	6.05	9.52×10^{-7}
0009605: Response to external stimulus	5.9	12.7	4.21×10^{-6}
0050896: Response to stimulus	16	25.8	4.24×10^{-6}
0031649: Heat generation	0.046	1.27	4.68×10^{-6}
0007052: Mitotic spindle organization and biogenesis	0.153	1.91	5.28×10^{-6}
0000226: Microtubule cytoskeleton organization and biogenesis	0.649	3.51	5.55×10^{-6}
0007010: Cytoskeleton organization and biogenesis	4.39	10.1	8.14×10^{-6}
0000067: DNA replication and chromosome cycle	0.0993	1.59	8.43×10^{-6}
0007051: Spindle organization and biogenesis	0.168	1.91	9.76×10^{-6}

ASC, adipose tissue-derived mesenchymal stem cells.

ing VEGF, HGF and SDF-1α.[4,5,10] To compare the proteins secreted by cultured ASC and BM-MSC, we used ELISA to investigate the production of several angiogenic and growth factors from ASC and BM-MSC cultures (**Figure 4**). As compared with BM-MSC, ASC secreted significantly larger amounts of not only HGF and VEGF, which are growth and angiogenic factors, but also PAI-1 and IL-6, which are adipokines. On the other hand, BM-MSC secreted significantly larger amounts of SDF-1α, which is a cell migration-related chemokine, than ASC. There was no significant difference between ASC and BM-MSC for several secreted adipokines, such as adiponectin and TNF-α.

Discussion

In this study, we examined the differences between ASC and BM-MSC in proliferation, differentiation, gene expression and secreted proteins. We showed that (1) ASC are more proliferative than BM-MSC, although there is no difference in differentiation into adipocytes or osteocytes; (2) genes associated with mitosis, inflammation and stress response are highly expressed in ASC; (3) genes associated with regulation of organ development, morphogenesis and cell migration are highly expressed in BM-MSC; and (4) ASC secrete significantly larger amounts of growth factors and inflammatory cytokines than BM-MSC, although BM-MSC secrete significantly larger amounts of chemokine than ASC.

In terms of differentiation, both ASC and BM-MSC differentiated into adipocytes and osteocytes, and there was no difference between them in adipogenesis in our quantitative analysis. A previous report demonstrated that BM-MSC had distinct osteogenic differentiation capability in comparison with ASC,[18] although we did not evaluate difference in osteogenesis between ASC and BM-MSC. Indeed, osteomodulin, which is an osteogenesis-related gene, was upregulated in BM-MSC in comparison with ASC (**Table 2**). Therefore, BM-MSC might have more osteogenic potential than ASC. These findings suggest that ASC and BM-MSC have multilineage potential and an equivalent potential to differentiate into unfavorable cells. Under these conditions, we found that ASC proliferated more rapidly than BM-MSC, and expanded 4-fold as much BM-MSC in approximately 2 weeks. Lee et al compared the proliferation and gene expression profile of human ASC and BM-MSC,[19] and also demonstrated that ASC differ from BM-MSC in terms of proliferation according to culture medium. A large number of MSC are needed for cell transplantation, so rapid proliferation of ASC ex vivo is thought to be a favorable source of transplanted cells in the acute clinical setting, although there remain prob-

Table 4. Classification of Highly (>3-Fold) Expressed Genes in BM-MSC According to Gene Ontology Terms

Category	% of genes in category	% of genes in list in category	P value
0048513: Organ development	8.86	21.9	5.02×10^{-12}
0008283: Cell proliferation	5.07	15.4	1.77×10^{-11}
0040007: Growth	2.18	9.62	4.23×10^{-11}
0009653: Morphogenesis	8.46	20.6	5.90×10^{-11}
0007275: Development	21.1	37.1	1.64×10^{-10}
0016049: Cell growth	1.53	7.56	6.82×10^{-10}
0016477: Cell migration	1.88	8.24	1.29×10^{-9}
0001558: Regulation of cell growth	1.31	6.52	8.83×10^{-9}
0007155: Cell adhesion	5.82	14.7	1.47×10^{-8}
0001501: Skeletal development	1.73	7.21	3.42×10^{-8}
0000902: Cellular morphogenesis	4.19	11.3	1.92×10^{-7}
0040008: Regulation of growth	1.64	6.52	3.21×10^{-7}
0009887: Organ morphogenesis	3.96	10.6	5.31×10^{-7}
0050678: Regulation of epithelial cell proliferation	0.0687	1.71	6.13×10^{-7}
0051674: Localization of cell	2.87	8.59	1.10×10^{-6}
0007626: Locomotory behavior	3.16	8.93	1.92×10^{-6}
0050673: Epithelial cell proliferation	0.084	1.71	2.17×10^{-6}
0006952: Defense response	6.27	13.7	2.26×10^{-6}
0009607: Response to biotic stimulus	6.59	14.1	3.12×10^{-6}
0045785: Positive regulation of cell adhesion	0.045	1.37	3.46×10^{-6}
0042127: Regulation of cell proliferation	3.32	8.93	4.56×10^{-6}
0050874: Organismal physiological process	16.7	27.1	4.75×10^{-6}

BM-MSC, bone marrow-derived mesenchymal stem cells.

lems concerning tumorigenesis and instability.

In this study, we carried out a comprehensive analysis in rat ASC and BM-MSC using microarrays. Interestingly, there was a considerable difference between the gene profile of our data and that of Lee et al,[19] who demonstrated that highly expressed genes in ASC accounted for less than 1% of all genes, and keratin 18, thrombospondin 1 and heat shock protein were included in the list of genes upregulated in ASC as compared with BM-MSC. Their human study was of 16–84-year-old patients undergoing arthroplasty and abdominoplasty, whereas we used 6-week-old rats. It is possible that differences in species and culture conditions, as well as age, contributed to these differences in gene expression.

We demonstrated that many of the genes that were highly expressed in ASC could be classified into categories such as mitosis, cell cycle and inflammatory cytokines, suggesting that ASC are more proliferative than BM-MSC. Thus, ASC transplant may not be superior to BM-MSC in terms of improvement of cardiac function in acute myocardial infarction, although it might be expected that ASC would contribute more to cell proliferation because of their secretion of VEGF and HGF. Also, ASC might initiate a stronger inflammatory response, because of the significantly increased upregulation of genes associated with inflammation as compared with BM-MSC. On the other hand, many of the genes that were highly expressed in BM-MSC were classified into categories such as organ development and morphogenesis. BM-MSC upregulated the expression of genes associated with cardiogenesis and angiogenesis, such as Wisp2, jagged1 and insulin-like growth factor binding protein 4 (IGFBP4). In particular, jagged1 and IGFBP4 have been reported to induce cardiogenesis and angiogenesis, respectively, via activation of notch signals and inhibition of Wnt signals.[20,21] Indeed, a previous report demonstrated that BM-MSC transplantation into the infarcted heart induces cardiogenesis and angiogenesis.[22–24] On the other hand, ASC are also reported to be able to differentiate into cardiomyocytes.[25] Therefore, ASC and BM-MSC both might improve cardiac function by supplementing cardiomyocytes, as well as in a paracrine manner, although we did not investigate differences in differentiation into cardiomyocytes between them.

BM-derived mononuclear cells and MSC have been used for therapeutic angiogenesis in ischemic disease.[26,27] MSC are thought to be more effective than mononuclear cells as a source of transplanted cells because MSC secrete larger amounts of growth factors.[26] Recent studies suggest that MSC exert tissue regeneration not only by differentiation into specific cell types, but also through paracrine actions, secreting various kinds of angiogenic and cytoprotective factors,[5,10] as shown in the present study. A recent report has shown that the combination of VEGF and MSC can enhance angiogenesis after acute myocardial infarction in rats.[28] Additionally, a previous study demonstrated that BM-MSC activate cardiac progenitor cells, which have the ability to differentiate into cardiomyocytes, in a paracrine manner in vitro and in vivo.[29,30] HGF and SDF-1α improve cardiac function via the activation of cardiac progenitor cells.[31] In our study, both ASC and BM-MSC secreted various cytokines and chemokines that are related to angiogenesis and cardiogenesis.

Although ASC are used as an adequate transplanted cell type for the treatment of ischemic limb disease,[32] ASC secrete larger amounts of not only inflammatory cytokines, such as IL-6, but also PAI-1 which promotes coagulation. In our gene analysis, several genes associated with other inflammatory cytokines and chemokines were upregulated in ASC. Not only the gene analysis but also the ELISA results suggested that ASC evoke more inflammation and thrombogenesis than BM-MSC. Therefore, ASC transplantation might be a more useful

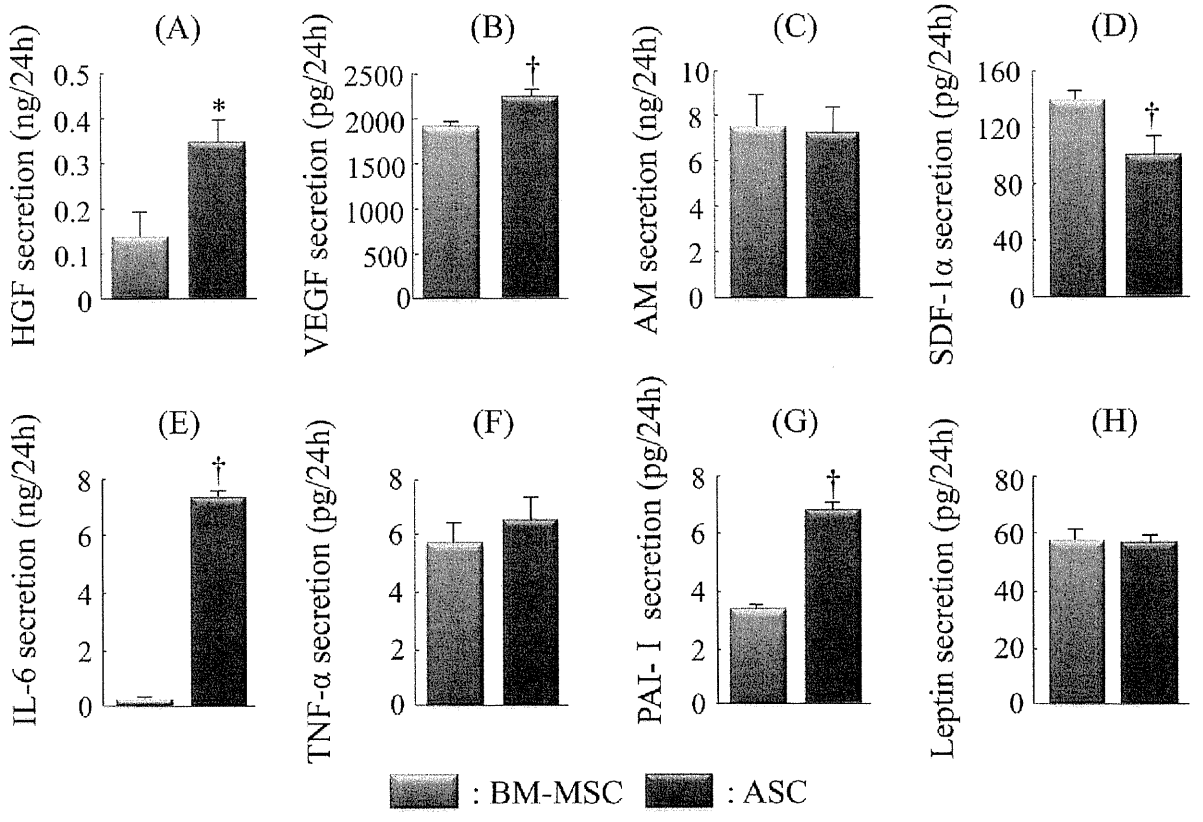

Figure 4. Secretory proteins from adipose tissue-derived mesenchymal stem cells (ASC: red) and bone marrow-derived mesenchymal stem cells (BM-MSC: blue). Conditioned media from ASC and BM-MSC were collected after incubation for 24h in complete medium. Hepatocyte growth factor (HGF, **A**), vascular endothelial growth factor (VEGF, **B**), adrenomedullin (AM, **C**), stem cell-derived factor-1α (SDF-1α, **D**), interleukin-6 (IL-6, **E**), tumor necrosis factor-α (TNF-α, **F**), plasminogen activator inhibitor-1 (PAI-1, **G**), and leptin (**H**) in conditioned media were measured by enzyme-linked immunosorbent assay. Values are mean±standard error of the mean. *P<0.05, †P<0.01 vs. BM-MSC.

treatment for chronic ischemia without severe inflammation.

In this study, we investigated ASC and BM-MSC obtained from young, 6-week-old rats, and we did not examine differences among various generations of rats. A previous report showed that MSC are subject to molecular genetic changes, such as alterations in p53, HGF and VEGF, during aging.[33] Our results might reflect the character of MSC obtained from young rats, contributing to difference from results in humans.[18] We need to further investigate differences between ASC and BM-MSC not only derived from rats but also derived from humans of various ages.

Conclusion

We have demonstrated difference in proliferation and gene expression between ASC and B-MSC, and accordingly, we suggest the importance of selecting the appropriate cell type for transplantation according to the therapeutic indication.

Acknowledgments

This work was supported by research grants for Human Genome Tissue Engineering 009 from the Ministry of Health, Labor and Welfare, and the Industrial Technology Research Grant Program from the New Energy and Industrial Technology Development Organization (NEDO) of Japan.

References

1. Pittenger MF, Mackay AM, Beck SC, Jaiswal RK, Douglas R, Mosca JD, et al. Multilineage potential of adult human mesenchymal stem cells. *Science* 1999; **284:** 143–147.
2. Minguell JJ, Erices A, Conget P. Mesenchymal stem cells. *Exp Biol Med* 2001; **226:** 507–520.
3. Prockop DJ. Marrow stromal cells as stem cells for nonhematopoietic tissues. *Science* 1997; **276:** 71–74.
4. Nagaya N, Fujii T, Iwase T, Ohgushi H, Itoh T, Uematsu M, et al. Intravenous administration of mesenchymal stem cells improves cardiac function in rats with acute myocardial infarction through angiogenesis and myogenesis. *Am J Physiol* 2004; **287:** 2670–2676.
5. Nagaya N, Kangawa K, Itoh T, Iwase T, Murakami S, Miyahara Y, et al. Transplantation of mesenchymal stem cells improves cardiac function in a rat model of dilated cardiomyopathy. *Circulation* 2005; **112:** 1128–1135.
6. Kinnaird T, Stabile E, Burnett MS, Shou M, Lee CW, Barr S, et al. Local delivery of marrow-derived stromal cells augments collateral perfusion through paracrine mechanisms. *Circulation* 2004; **109:** 1543–1549.
7. Chen S, Liu Z, Tian N, Zhang J, Yei F, Duan B, et al. Intracoronary transplantation of autologous bone marrow mesenchymal stem cells for ischemic cardiomyopathy due to isolated chronic occluded left anterior descending artery. *J Invasive Cardiol* 2006; **18:** 552–556.
8. Chen SL, Fang WW, Ye F, Liu YH, Qian J, Shan SJ, et al. Effect on left ventricular function of intracoronary transplantation of autologous bone marrow mesenchymal stem cell in patients with acute myocardial infarction. *Am J Cardiol* 2004; **94:** 92–95.
9. De Ugarte DA, Morizono K, Elbarbary A, Alfonso Z, Zuk PA, Zhu

M, et al. Comparison of multi-lineage cells from human adipose tissue and bone marrow. *Cells Tissues Organs* 2003; **174:** 101–109.
10. Kinnaird T, Stabile E, Burnett MS, Lee CW, Barr S, Fuchs S, et al. Marrow-derived stromal cells express genes encoding a broad spectrum of arteriogenic cytokines and promote in vitro and in vivo arteriogenesis through paracrine mechanisms. *Circ Res* 2004; **94:** 678–685.
11. Zuk PA, Zhu M, Mizuno H, Huang J, Futrell JW, Katz AJ, et al. Multilineage cells from human adipose tissue: Implications for cell-based therapies. *Tissue Eng* 2001; **7:** 211–228.
12. Miyahara Y, Nagaya N, Kataoka M, Yanagawa B, Tanaka K, Hao H, et al. Monolayered mesenchymal stem cells repair scarred myocardium after myocardial infarction. *Nature Med* 2006; **12:** 459–465.
13. Moon MH, Kim SY, Kim YJ, Kim SJ, Lee JB, Bae YC, et al. Human adipose tissue-derived mesenchymal stem cells improve postnatal neovascularization in a mouse model of hindlimb ischemia. *Cell Physiol Biochem* 2006; **17:** 279–290.
14. Gronthos S, Franklin DM, Leddy HA, Robey PG, Storms RW, Gimble JM. Surface protein characterization of human adipose tissue-derived stromal cells. *J Cell Physiol* 2001; **189:** 54–63.
15. Wakitani S, Saito T, Caplan AI. Myogenic cells derived from rat bone marrow mesenchymal stem cells exposed to 5-azacytidine. *Muscle Nerve* 1995; **18:** 1417–1426.
16. Solchaga LA, Penick K, Porter JD, Goldberg VM, Caplan AI, Welter JF. FGF-2 enhances the mitotic and chondrogenic potentials of human adult bone marrow-derived mesenchymal stem cells. *J Cell Physiol* 2005; **203:** 398–409.
17. Ohnishi S, Yasuda T, Kitamura S, Nagaya N. Effect of hypoxia on gene expression of bone marrow-derived mesenchymal stem cells and mononuclear cells. *Stem Cells* 2007; **25:** 1166–1177.
18. Hayashi O, Katsube Y, Hirose M, Ohgushi H, Ito H. Comparison of osteogenic ability of rat mesenchymal stem cells from bone marrow, periosteum, and adipose tissue. *Calcif Tissue Int* 2008; **82:** 238–247.
19. Lee RH, Kim B, Choi I, Kim H, Choi HS, Suh K, et al. Characterization and expression analysis of mesenchymal stem cells from human bone marrow and adipose tissue. *Cell Physiol Biochem* 2004; **14:** 311–324.
20. Zhu W, Shiojima I, Ito Y, Li Z, Ikeda H, Yoshida M, et al. IGFBP-4 is an inhibitor of canonical Wnt signalling required for cardiogenesis. *Nature* 2008; **454:** 345–349.
21. Boni A, Urbanek K, Nascimbene A, Hosoda T, Zheng H, Delucchi F, et al. Notch1 regulates the fate of cardiac progenitor cells. *Proc Natl Acad Sci USA* 2008; **105:** 15529–15534.
22. Tang XL, Rokosh DG, Guo Y, Bolli R. Cardiac progenitor cells and bone marrow-derived very small embryonic-like stem cells for cardiac repair after myocardial infarction. *Circ J* 2010; **74:** 390–404.
23. Hosoda T, Kajstura J, Leri A, Anversa P. Mechanisms of myocardial regeneration. *Circ J* 2010; **74:** 13–17.
24. Tsubokawa T, Yagi K, Nakanishi C, Zuka M, Nohara A, Ino H, et al. Impact of anti-apoptotic and -oxidative effects of bone marrow mesenchymal stem cells with transient overexpression of heme oxygenase-1 on myocardial ischemia. *Am J Physiol* 2010; **298:** 1320–1329.
25. Choi YS, Dusting GJ, Stubbs S, Arunothayaraj S, Han XL, Collas P, et al. Differentiation of human adipose-derived stem cells into beating cardiomyocytes. *J Cell Mol Med* 2010; **14:** 878–889.
26. Iwase T, Nagaya N, Fujii T, Itoh T, Murakami S, Matsumoto T, et al. Comparison of angiogenic potency between mesenchymal stem cells and mononuclear cells in a rat model of hindlimb ischemia. *Cardiovasc Res* 2005; **66:** 543–551.
27. Kinnaird T, Stabile E, Burnett MS, Epstein SE. Bone-marrow-derived cells for enhancing collateral development: Mechanisms, animal data, and initial clinical experiences. *Circ Res* 2004; **95:** 354–363.
28. Tang J, Wang J, Zheng F, Kong X, Guo L, Yang J, et al. Combination of chemokine and angiogenic factor genes and mesenchymal stem cells could enhance angiogenesis and improve cardiac function after acute myocardial infarction in rats. *Mol Cell Biochem* 2010; **339:** 107–118.
29. Nakanishi C, Yamagishi M, Yamahara K, Hagino I, Mori H, Sawa Y, et al. Activation of cardiac progenitor cells through paracrine effects of mesenchymal stem cells. *Biochem Biophys Res Commun* 2008; **374:** 11–16.
30. Hatzistergos KE, Quevedo H, Oskouei BN, Hu Q, Feigenbaum GS, Margitich IS, et al. Bone marrow mesenchymal stem cells stimulate cardiac stem cell proliferation and differentiation. *Circ Res* 2010; **107:** 913–922.
31. Rota M, Padin-Iruegas ME, Misao Y, De Angelis A, Maestroni S, Ferreira-Martins J, et al. Local activation or implantation of cardiac progenitor cells rescues scarred infarcted myocardium improving cardiac function. *Circ Res* 2008; **103:** 107–116.
32. Bhang SH, Cho SW, Lim JM, Kang JM, Lee TJ, Yang HS, et al. Locally delivered growth factor enhances the angiogenic efficacy of adipose-derived stromal cells transplanted to ischemic limbs. *Stem cells* 2009; **27:** 1976–1986.
33. Wilson A, Shehadeh LA, Yu H, Webster KA. Age-related molecular genetic changes of murine bone marrow mesenchymal stem cells. *BMC Genomics* 2010; **229:** 7–11.

International Journal of Cardiology xxx (2011) xxx–xxx

Contents lists available at ScienceDirect

International Journal of Cardiology

journal homepage: www.elsevier.com/locate/ijcard

Analysis of liver metabolism in a rat model of heart failure☆

Takao Kato [a,b], Shinichiro Niizuma [a], Yasutaka Inuzuka [a], Tsuneaki Kawashima [a], Junji Okuda [a], Akira Kawamoto [a], Yodo Tamaki [a], Yoshitaka Iwanaga [a], Tomoyoshi Soga [c], Toru Kita [a], Takeshi Kimura [a], Tetsuo Shioi [a,*]

[a] Department of Cardiovascular Medicine, Graduate School of Medicine, Kyoto University, Kyoto, Japan
[b] Division of Cardiology, The Tazuke Kofukai Medical Reseach Institute, Kitano Hospital, Osaka, Japan
[c] Institute for Advanced Bioscience, Keio University, Yamagata, Japan

ARTICLE INFO

Article history:
Received 28 December 2010
Received in revised form 5 July 2011
Accepted 10 July 2011
Available online xxxx

Keywords:
Heart failure
Cachexia
Liver
Lipogenesis
Inflammation

ABSTRACT

Background: Cachexia, namely body wasting, is a common complication in cases of congestive heart failure (CHF). Although, neurohumoral and immune abnormalities are associated with the condition, precisely how the imbalance of catabolism and anabolism is responsible for the wasting process is not known.
Methods: We analyzed markers of cachexia in Dahl salt-sensitive rats which show marked hypertension with preserved systolic function at 11 weeks and CHF at 17–19 weeks of age. We also analyzed the change in hepatic metabolism associated with CHF since liver plays a central role in the systemic regulation of catabolism and anabolism.
Results: In CHF rats, a failure to grow was observed and blood hepatic protein levels were decreased associated with increased blood proinflammatory cytokine levels, indicating that Dahl rats serve as a model of cardiac cachexia. Food intake was reduced, and blood sugar and insulin levels were decreased. Despite the apparent fasting condition, blood fatty acid levels were decreased and triglycerides levels were increased. In CHF rats, liver incorporated more glucose, the gene expression related to gluconeogenesis was decreased, the gene expression related to lipogenesis was increased, and the triglyceride content of the liver was increased. The paradoxical production of triglycerides synthesis in fasting rats was associated with a proinflammatory response in liver.
Conclusions: The Dahl salt-sensitive rat can be used as a model of cardiac cachexia. The cachexia was associated with abnormal hepatic metabolism that might work as a maladaptive response during the progression of CHF.

1. Introduction

Congestive heart failure (CHF) is becoming a serious health care problem. CHF is associated with a significant change in energy metabolism of the heart, and the altered energetics is hypothesized to play an important role in the progression of CHF [1]. Using a Dahl rat model which shows a distinct transition from compensated left ventricular hypertrophy to CHF, we recently found that left ventricular hypertrophy or CHF was associated with a distinct change in the metabolic profile of the heart and that the metabolic remodeling of heart might be a therapeutic target [2].

CHF is also associated with abnormal energy metabolism in extracardiac tissues. Cachexia, namely body wasting, is a common complication among CHF patients [3,4]. Cardiac cachexia is associated with a poor prognosis and disability. Several lines of evidence suggest that neurohumoral and immune abnormalities play a critical role, and a complex imbalance of catabolism and anabolism is likely to be responsible for the development of the wasting process [4].

Although cardiac cachexia is an important complication and a potential target of therapeutic intervention in cases of CHF, its pathophysiology is poorly understood. One reason for this is the limited number of animal models of cardiac cachexia available. There is a report that the skeletal muscle atrophy caused by reduced activity is significantly different from the muscle atrophy observed in CHF rats [5]. However, the mechanism by which the imbalance between catabolism and anabolism is induced is not clear. In this study, we have shown that the Dahl salt-sensitive rat fed a high-salt diet is an animal model of cardiac cachexia. To gain insight into the mechanism of cardiac cachexia, we have analyzed the change of hepatic

☆ Grant support: Grants from the Japan Society for the Promotion of Science, Japan Heart Foundation, Japan Foundation of Cardiovascular Research, NOVARTIS Foundation for the Promotion of Science, Mochida Memorial Foundation for Medical and Pharmaceutical Research, Takeda Science Foundation, and Vehicle Racing Commemorative Foundation.

* Corresponding author at: Department of Cardiovascular Medicine, Graduate School of Medicine, Kyoto University, 54 Shogoinkawahara-cho, Sakyo-ku, Kyoto 606-8507, Japan. Tel.: +81 75 751 3670; fax: +81 75 751 3203.
E-mail address: tshioi@kuhp.kyoto-u.ac.jp (T. Shioi).

0167-5273/$ – see front matter © 2011 Elsevier Ireland Ltd. All rights reserved.
doi:10.1016/j.ijcard.2011.07.056

Table 1
Primer sequences used in real time quantitative RT-PCR.

Gene	Forward	Reverse	Ref.	GenBank entry
18SrRNA	AGTCCCTGCCCTTTGTACACA	CGATCCGAGGGCCTCACTA	[26]	M11188
Pyruvate carboxylase	CCGTTCTAAGGTGCTAAAGGA	GACGAGTATTCAGGCTATCCA		BC085680.1
Phosphoenolpyruvate carboxykinase (PEPCK)	ATGTCAGAAGAGGACTTCGAGA	CTCAATACCAATCTTGGCCAGA		BC085680.1
ATP Citrate lyase	GGCAAGATCCTCATCATTGGA	CAACTTCTCCCATCACTCGTA		BC100618.1
Acetyl-CoA carboxylase (ACC) α	ATGATTGCTGGGGAATCCTCA	GAGGTGTATACTTCCCGACCA		NM_022193.1
Fatty acid synthase	CAAGTTATTCGACCACCCAGA	TCACCCAGTTGTCTTTCCAGA		NM_017332.1
Sterol regulatory element-binding protein (SREBP) 1c	TCACTGAAAGACCTGGTGTCA	GCTTTCACCTGGTTATCCTCA		AF286470.2
Sterol regulatory element-binding protein (SREBP) 2	CAAGTACCTGCAGCAGGTCA	AGTCAATGGAATAGGGGGAGA		NM_001033694
Tumor necrosis factor (TNF)α	ATGGTCCTCTTTCAGTCG GAG	TGTC TACTGAACTTCGGGGTG	[27]	NM_012675.3
Interleukin (IL)1β	CTTCCCCAGGACATGCTAGG	CAAAGGCTTCCCCTGGAGAC	[28]	NM_031512.2
C-reactive protein (CRP)	ACATTGTGGGGACAAATGCA	ACATTGGGGCTGAATACCCTA		NM_017096.3
Transthyretin	GGCTCACCACAGATGAGAAGTTC	ACAAATGGGAGCTACTGCTTTGGC	[29]	NM_012681.1
Retinol-binding protein (RBP) 4	AGAAGGGTCATATGAGCGCTA	GTATCGATGATCCAGTGGTCA		NM_013162.1
Hepatocyte nuclear factor (HNF) 4	AAATGTGCAGGTGTTGACCA	CACGCTCCTCCTGAAGAATC	[29]	EF193392

metabolism since the liver plays a central role in the systemic regulation of catabolism and anabolism.

2. Materials and methods

2.1. Animals

Inbred male Dahl salt-sensitive (DS) rats (Japan SLC, Hamamatsu, Shizuoka, Japan) were fed a 0.3% NaCl (low salt; LS) diet until the age of 6 weeks, then an 8% NaCl (high salt; HS) diet [2]. DS rats fed only the low-salt diet were used as controls. Animal care and the experiments were approved by the Institutional Animal Care and Use Committee of Kyoto University and conducted by the Guide for the Care and Use of Laboratory Animals published by the United States National Institutes of Health.

2.2. Protocols

Serial measurements of body weight, food intake, and cardiac function by echocardiography were performed from 11 weeks of age. Blood samples were obtained at age 18 weeks without fasting. The measurement of mRNAs, proteins, and metabolites was performed at the age of 11 and 18 weeks without fasting. The hepatic uptake of ^{18}F-deoxyglucose (FDG) and ^{125}I-15-(*p*-iodophenyl)-9-*R*,*S*-methylpentadecanoic acid (9MPA) was measured at age 11 and 18 weeks after an overnight fast.

2.3. Cardiac echocardiography

Echocardiography was performed based on a previously reported protocol [2]. Briefly, rats were anesthetized with inhaled diethyl ether (Wako Pure Chemical Industries, Osaka, Japan), and transthoracic echocardiography was performed using a Sonos-5500 echocardiograph (Agilent Technologies, Santa Clara, CA) with a 15-MHz linear transducer. M-mode echocardiograms were obtained at the papillary muscle level. At least two independent M-mode measurements for each animal were carried out.

2.4. Blood analysis

Blood samples were collected without fasting via the right ventricle, and the samples were centrifuged at 3000 rpm for 15 min and analyzed as described [2]. Plasma concentration of insulin was analyzed using a commercial kit (Shibayagi Co., Shibukawa, Gunma, Japan).

2.5. Sampling of hepatic tissue

To obtain liver tissues for biochemical analyses, 11-week-old LS (n=6), 11-week-old HS (n=8), and 17-week-old HS (n=6) rats were sacrificed by decapitation without fasting. A piece of the liver was obtained from the right lobe, rapidly divided, snap frozen in liquid nitrogen, and stored at −80 °C. The liver tissues were also used for the measurement of mRNA, glycogen, and triglyceride (TG).

2.6. Metabolome analysis (CE-TOFMS)

A targeted metabolomic approach was performed using capillary electrophoresis time-of-flight mass spectrometry (CE-TOFMS) [6]. Hepatic tissue from 11-week-old LS (n=6), 11-week-old HS (n=6), and 17-week-old HS (n=6) rats were analyzed. The conditions used were described in Supplementary materials.

2.7. Levels of glycogen and triglycerides

Glycogen and TGs were extracted from liver tissue of 11-week-old LS, 11-week-old HS, and 17-week-old HS rats (n=6–8 in each group) using previously described methods [7,8], and analyzed with commercial kits (BioAssay Systems, Hayward, CA, and Cayman Chemical, Ann Arbor, MI, respectively).

2.8. Quantitative reverse transcription-polymerase chain reaction (RT-PCR)

Total RNA was isolated from the liver tissue (n=6–8 in each group) by the acid guanidinium thiocyanate–phenol–chloroform method. Quantitative RT-PCR was carried out as described previously [2]. The sequences of primers used are listed in Table 1. The mRNA level of each gene was standardized with the corresponding 18S ribosomal RNA as an internal control. The Genbank accession numbers are also included in Table 1.

2.9. Western blotting

Liver lysate was obtained by homogenization in ice-cold buffer [10% glycerol, 137 mM NaCl, 20 mM Tris–HCl pH 7.4, 4 g/ml aprotinin, 4 g/ml leupeptin, 1 mM phenylmethylsulfonyl fluoride (PMSF), 4 g/ml pepstatin, 20 mM NaF, 1 mM sodium pyrophosphate, and 1 mM orthovanadate] [9]. The lysate was kept on ice for 15 min and cleared by centrifugation at 15,000 g for 20 min at 4 °C. Protein concentrations were determined by the Bradford method (BioRad, Hercules, CA). 200 μg of liver tissue lysate was subjected to sodium dodecyl sulfate-polyacrylamide gel electrophoresis (SDS-PAGE), and the proteins were transferred onto polyvinylidene difluoride membranes. The primary antibodies used for western blotting were for sterol regulatory element-binding protein (SREBP) 1 (2A4, 1:500, Santa Cruz, Santa Cruz, CA), SREBP2

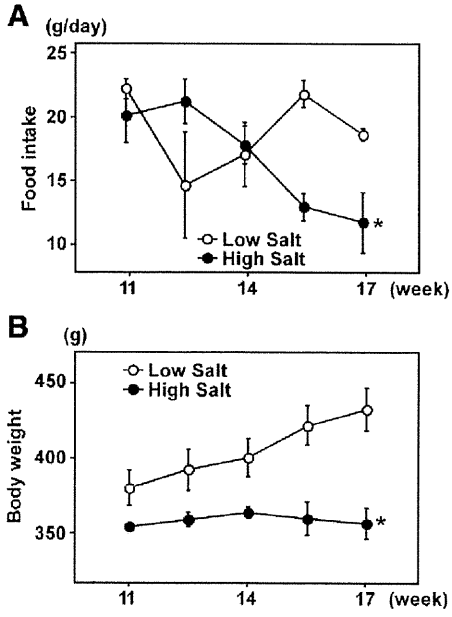

Fig. 1. Food intake and body weight of Dahl rats fed a high-salt diet. (A) Serial measurements of food intake. Rats with congestive heart failure (CHF) ate less than control rats. (B) Serial measurements of body weight. CHF rats showed a failure to grow. n=4 for each group. *p<0.05 versus control rats, namely Dahl rats fed a low-salt diet.

Please cite this article as: Kato T, et al, Analysis of liver metabolism in a rat model of heart failure, Int J Cardiol (2011), doi:10.1016/j.ijcard.2011.07.056

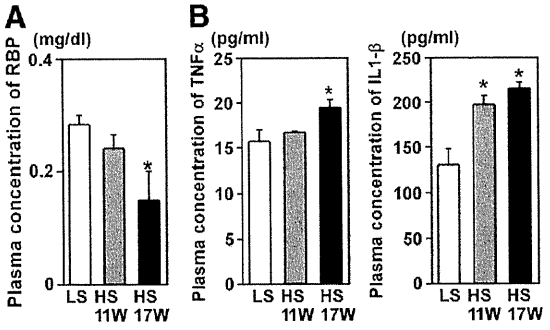

Fig. 2. Markers of cachexia in Dahl rats. (A) The concentration of retinol-binding protein (RBP) in plasma was decreased in CHF rats (HS 17W). (B) The plasma concentration of tumor necrosis factor (TNF)-α and interleukin (IL)1-β was increased in CHF rats. n = 6–8 in each group. LS; low salt, HS; high salt. *p<0.05 versus control LS rats.

(1:500, (Cayman Chemical), and glyceraldehyde-3-phosphate dehydrogenase (GAPDH; 1:1000, Chemicon, Temecula, CA).

2.10. Hepatic uptake of ^{18}FDG and ^{125}I-9MPA

The hepatic uptake of glucose and fatty acids was estimated by measuring the incorporation of an analog of glucose (deoxyglucose) and a fatty acid (9MPA) as described [2]. The 11-week-old LS (n = 7), 11-week-old HS (n = 10), and 17-week-old HS rats (n = 12) were injected with 1 mCi of ^{18}FDG and 20 μCi of ^{125}I-9MPA. The animals were fasted overnight before the injection since variation in the uptake of the isotope-labeled molecule was found when fed animals were used. The rats were sacrificed by decapitation 45 min after the injection, and the livers were removed and washed in cold saline. Specimens of the left lobe were collected and frozen in liquid nitrogen and radioisotopic activity was measured using a scintillation counter (Packard Cobra2 ™ Auto-gamma, GMI, Ramsey, Minnesota) [2]. To measure ^{18}FDG uptake, radioisotopic activity was measured just after sacrifice because the half decay time of ^{18}FDG is 110 min. To measure ^{125}I-9MPA uptake, another radioisotopic measurement was made 48 h after the first. The amount of radioisotope incorporated was presented as a percentage of the administered dose corrected by liver weight in grams. Using this method, cross-talk between the two tracers was negligible [2].

2.11. Plasma and tissue concentrations of inflammatory cytokines

The levels of tumor necrosis factor (TNF)-α and interleukin (IL)1-β in tissue homogenate and plasma were measured using sandwich enzyme-linked immunosorbent assay (ELISA) kits (Shibayagi Co. and R&D Systems; Minneapolis, MN), according to the manufacturers' instructions. The tissue homogenate for the protein analysis was used in this assay.

2.12. Statistical analysis

Values are expressed as means ± SEMs. Differences among experimental groups were tested by ANOVA with post hoc comparisons using the Bonferroni test. In all tests, a value of $p<0.05$ was considered significant.

3. Results

3.1. Dahl rats fed a high-salt diet develop hypertension, heart failure, and cachexia

As we reported previously, DS rats fed a high-salt (HS) diet developed hypertension (HT) at 11 weeks of age (systolic blood pressure; 211 ± 12 mm Hg, diastolic blood pressure; 160 ± 6 mm Hg) [2]. On echocardiographic examination, fractional shortening (FS) was

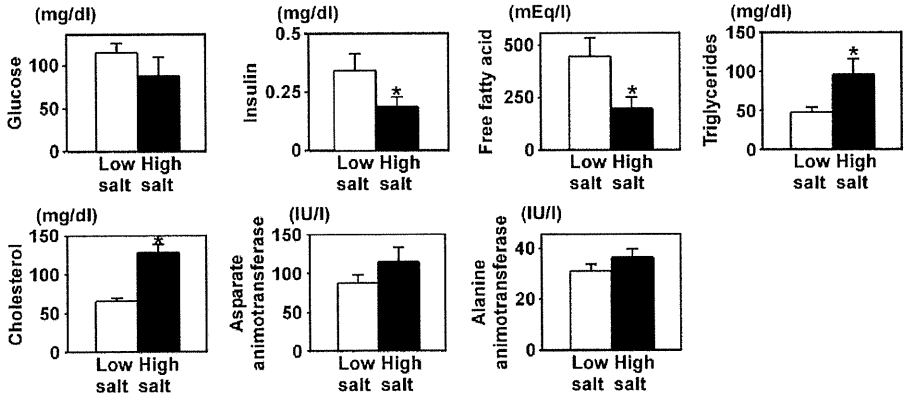

Fig. 3. Blood analysis of Dahl rats. Blood sugar and insulin levels were decreased, and triglyceride and cholesterol levels were increased in CHF rats. n = 5–6 in each group. *p<0.05 versus control rats.

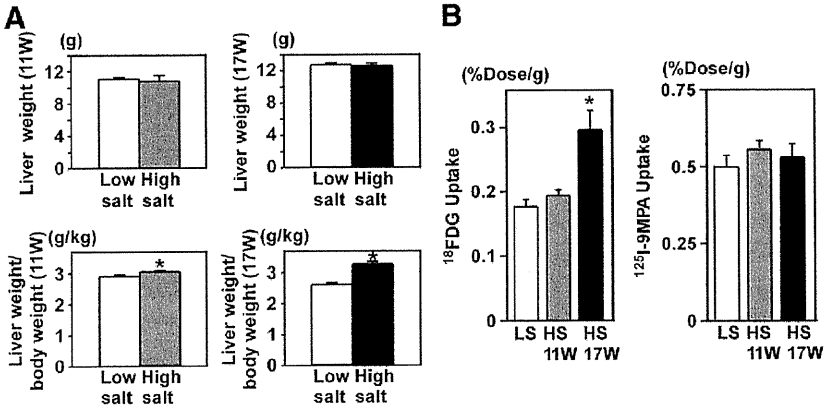

Fig. 4. Liver weight and the uptake of glucose and fatty acids. (A) Liver weight and liver weight corrected by body weight at 11 and 17 weeks of age. Liver weight corrected by body weight was increased in CHF rats (HS 17W) compared with control rats. n = 6–12 in each group. LS; low salt, HS; high salt. *p<0.05 versus control rats. (B) The uptake of ^{18}FDG, a glucose analog, was increased in CHF rats (HS 17W) compared to control rats. The uptake of ^{125}I-9MPA, a fatty acid analog, in the liver was not changed. n = 7–12 in each group. *p<0.05 versus control rats.

Please cite this article as: Kato T, et al, Analysis of liver metabolism in a rat model of heart failure, Int J Cardiol (2011), doi:10.1016/j.ijcard.2011.07.056

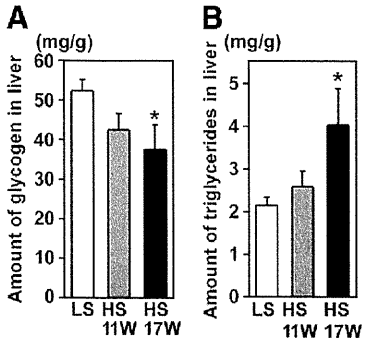

Fig. 5. Glycogen and triglyceride content in liver. (A) The amount of glycogen in liver was decreased in CHF rats. (B) The amount of triglycerides in liver was increased in CHF rats. n = 6–8 in each group. LS; low salt, HS; high salt. *p<0.05 versus control rats.

found to be preserved (62.4 ± 0.9%). At around 17 weeks of age, the rats showed signs of CHF, such as tachypnea and immobilization, and decreased FS (39.7 ± 1.5%). DS rats fed a low-salt (LS) diet did not develop hypertension or CHF, and were used as controls.

Serial measurements of food intake and body weight showed that CHF rats ate less than controls (Fig. 1A) and had a lower body weight (Fig. 1B). The failure to grow in the CHF rats led us hypothesize that the animals may serve as a model of cardiac cachexia. Blood levels of hepatic proteins, such as albumin, transthyretin, and transferrin, can serve as markers of a nutritional index to screen for malnutrition and monitor the metabolic response to dietary intervention [10,11]. Blood hepatic proteins are synthesized mainly in liver and have short half lives in blood. We measured the concentration of retinol-binding protein (RBP), a blood hepatic protein, in plasma and found that it was decreased in CHF rats (Fig. 2A). Cachexia is also known to be associated with neurohumoral and immune abnormalities [4]. Indeed, plasma concentrations of two representative proinflammatory cytokines, TNF-α and IL-1β, were elevated in CHF rats (Fig. 2B).

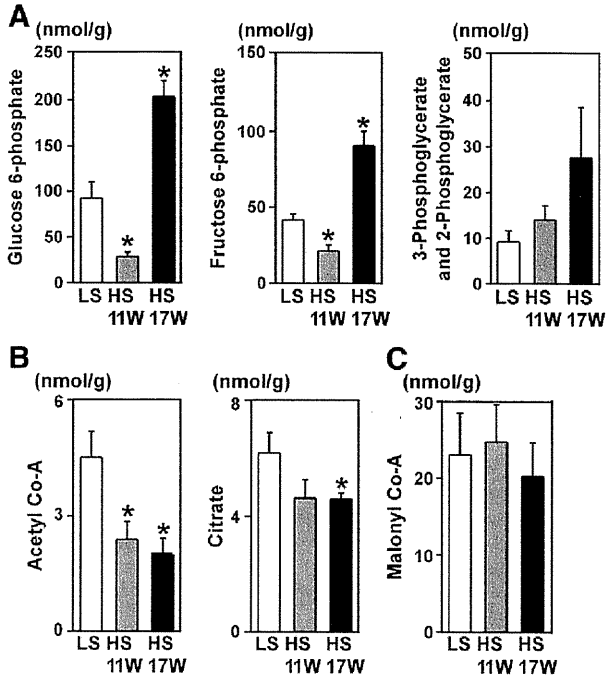

Fig. 6. The amounts of metabolites in liver determined by metabolome analysis. (A) Concentrations of metabolites of glycolysis. (B) Concentrations of metabolites in the Krebs cycle. (C) Malonyl CoA concentration. n = 6 in each group. LS; low salt, HS; high salt. *p<0.05 versus control rats.

3.2. Blood analysis of CHF rats

To investigate the systemic metabolic profile of Dahl rats, we examined blood chemistry. Both glucose and insulin levels were lower in CHF rats than control rats in the fed condition (Fig. 3), as reported [2]. Plasma levels of cholesterol and TG were increased, and free fatty acids (FFAs) were decreased in DS rats with CHF, as reported [2]. Concentrations of representative liver enzymes, such as aspartate amino transferase and alanine transaminase, did not differ among the groups. Lower food intake, associated with lower glucose and insulin levels, suggested that the animals were starved. However, the plasma level of FFAs was decreased and that of TG increased, which is not consistent with a starved condition. Based on these observations, we sought to examine the hepatic metabolism in this model since the liver plays a key role in the homeostasis of systemic catabolism and anabolism.

3.3. Analysis of energy metabolic pathways in the liver

Liver weight corrected by body weight was increased in CHF rats compared with control rats (Fig. 4A). The increase in liver weight is likely to be due to congestion since venous dilation in liver tissue is reported in this model [12]. It is of interest that increased right atrial pressure is reported to indicate malnutrition in CHF patients [13]. Despite lower blood sugar levels, the uptake of ^{18}FDG increased in CHF rats (Fig. 4B). The uptake of ^{125}I-9MPA, a fatty acid analog, was not changed (Fig. 4B). The amount of glycogen in liver was decreased, and that of TG was increased in the CHF rats (Fig. 5A, B). The metabolome analysis (Supplementary table) revealed that levels of some metabolites of glycolysis increased (Fig. 6A) and some metabolites in the Krebs cycle, such as acetyl-CoA and citrate, were decreased (Fig. 6B). Overall, these results may suggest hepatic lipogenesis to be increased and acetyl-CoA to be used for the synthesis of TG and cholesterol.

Next, we examined the gene expression related to lipogenesis and gluconeogenesis. The gene expression of enzymes related to lipogenesis, such as ATP citrate lyase, acetyl-CoA carboxylase, and fatty acid synthase, was up-regulated in CHF rats (Fig. 7A). In contrast, the expression of rate-limiting enzymes in gluconeogenesis, such as pyruvate carboxylase and phosphoenolpyruvate carboxykinase (PEPCK), was down-regulated. Next, we examine the expression of sterol regulatory element-binding protein (SREBP1)1-c and SREBP2, which increase lipogenesis and suppress gluconeogenesis [14,15]. The gene expression of SREBP1-c and SREBP2 was increased in CHF rats. The amount of SERBP proteins was also increased (Fig. 7B and C).

3.4. Expression of rapid turnover protein in liver

Since RBP, a blood hepatic protein, was decreased in the blood of CHF rats, we examined the gene expression of serum hepatic proteins. mRNA levels of transthyretin and retinol-binding protein (RBP) 4 were decreased in CHF rats (Fig. 8A). To examine the mechanism responsible for the decrease of rapid turnover proteins, we measured the expression of hepatocyte nuclear factor (HNF) 4. HNF4 is known to regulate transthyretin gene expression [16,17]. HNF4 mRNA levels started to decrease in rats with HT, and decreased significantly in rats with CHF (Fig. 8B).

3.5. Expression of proinflammatory genes

Inflammatory responses are reported to enhance lipogenesis [18] and induce cachexia [19]. It is well established that CHF is associated with the inflammation of cardiac and extra-cardiac tissue [20]. Thus, local inflammatory responses might be a mechanism causing

Please cite this article as: Kato T, et al, Analysis of liver metabolism in a rat model of heart failure, Int J Cardiol (2011), doi:10.1016/j.ijcard.2011.07.056

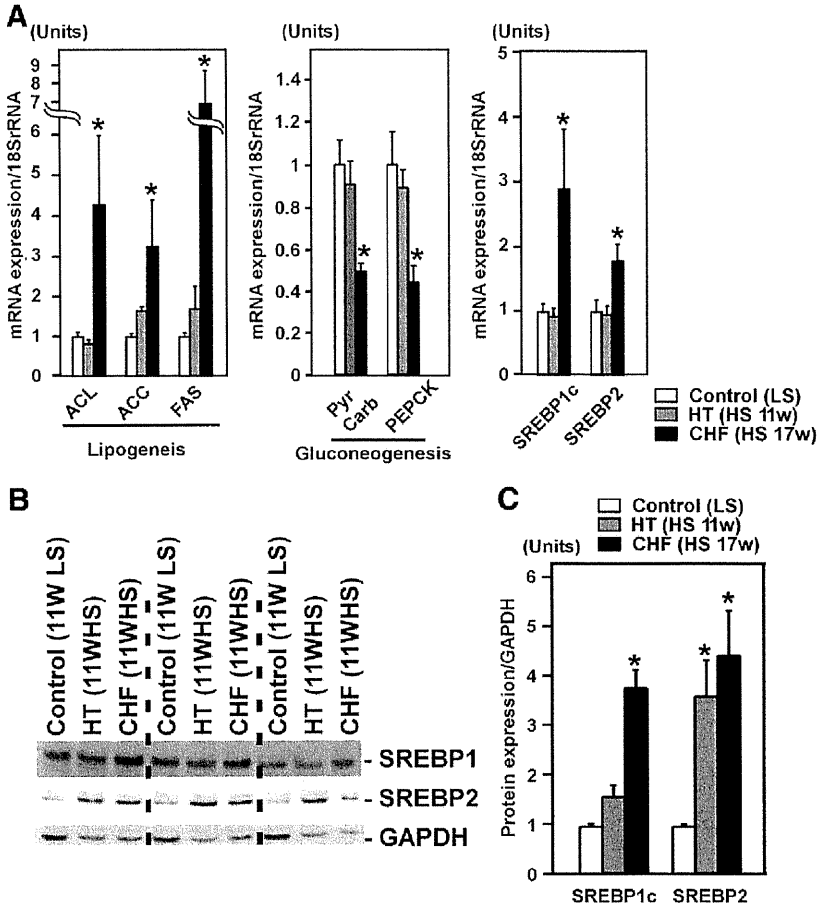

Fig. 7. Expression of mRNA and protein levels related to lipogenesis and gluconeogenesis. (A) The gene expression related to lipogenesis was increased in liver of CHF rats (HS 17W). The gene expression related to gluconeogenesis was decreased. The gene expression of sterol regulatory element-binding protein (SREBP)1c and SREBP2 was increased. n = 6–8 in each group. *p<0.05 versus control rats. (B) Representative images of the Western blotting of SREBP1 and SREBP2. (C) The protein levels of SREBP1 and SREBP2 in liver tissue were increased. n = 3 in each group. LS; low salt, HS; high salt. *p<0.05 versus control rats.

increased lipogenesis and the decreased synthesis of blood hepatic proteins. Therefore, we examined the expression of genes related to proinflammatory responses. The gene expression of TNF-α, IL1-β, and C-reactive protein, started to increase in liver of rats with HT but not with CHF, and significantly increased in CHF (Fig. 9A). The protein levels of TNF-α and interleukin1-β in liver also started to increase in HT rats, and remained increased in CHF rats (Fig. 9B).

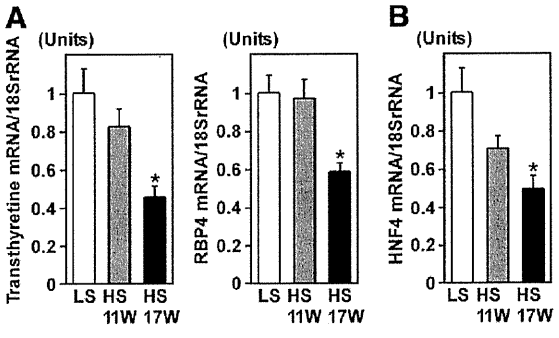

Fig. 8. Analysis of gene expression of hepatic proteins. (A) The gene expression of hepatic proteins, transthyretin and RBP4, was decreased in CHF rats (HS 17W). (B) Hepatocyte nuclear factor (HNF) 4 mRNA was decreased in CHF rats. n = 6–8 in each group. LS; low salt, HS; high salt. *p<0.05 versus control rats.

4. Discussion

In this study, we have shown that Dahl rat fed a high-salt diet developed CHF associated with a failure to grow, decreased blood hepatic protein, and increased blood proinflammatory cytokines. These results indicate the Dahl rat with CHF to be a model of cardiac cachexia.

4.1. Abnormal lipid metabolism in liver of CHF rats

During fasting, liver metabolism changes from anabolism to catabolism. Glucose is produced from glycogen breakdown and gluconeogenesis, and lipid accumulated as TG is used to produce FFAs. The glucose and FFAs are released into the circulation and delivered to the brain, skeletal muscle, the heart etc. However, despite decreased food intake and lower blood sugar and insulin levels, lipogenesis was increased in the liver of CHF rats (Fig. 10). The mechanism by which lipogenesis is increased on fasting in these rats is unknown. However, Fon Tacer et al. reported that giving TNF-α to fasted mice changed the metabolic profile of the liver from lipid usage to synthesis [18]. In that report, SREBP levels were are decreased in fasted mice, but increased on addition of TNF-α, associated with increased lipogenesis. Another report also showed abnormal lipid metabolism to be associated with inflammatory responses in liver [21]. Indeed, SREBPs increased in association with the amount of TNF-α mRNA and protein in this study. The TNF-α concentration in

Please cite this article as: Kato T, et al, Analysis of liver metabolism in a rat model of heart failure, Int J Cardiol (2011), doi:10.1016/j.ijcard.2011.07.056

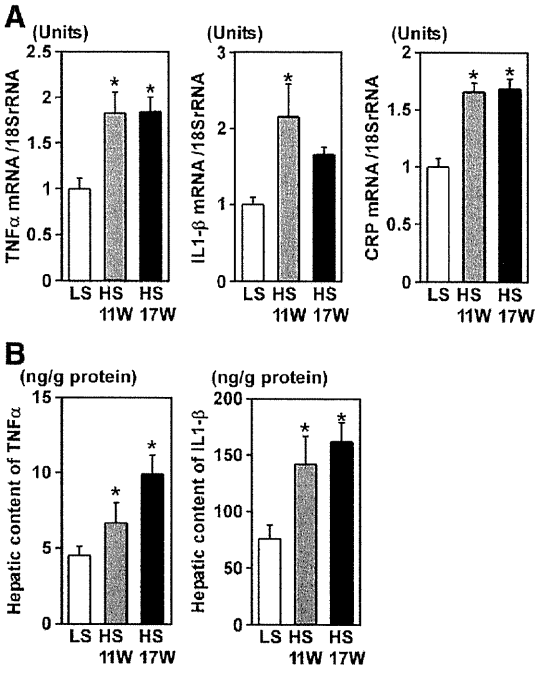

Fig. 9. Expression of proinflammatory cytokines in liver. (A) The gene expression of proinflammatory cytokines, TNF-α, IL1-β, and C-reactive protein (CRP), was increased in HT (HS 11W) and CHF rats (HS 17W). n = 6–8 in each group. (B) The amounts of TNF-α and IL1-β started to increase in the liver in HT rats, and remained increased in the liver in CHF rats assessed by ELISA. n = 6 in each group. LS; low salt, HS; high salt. *p<0.05 versus control rats.

liver was reported to be increased in an animal model of pacing-induced heart failure [22]. Thus, CHF-associated proinflammatory responses may be a mechanism of abnormal lipid metabolism in CHF rats.

4.2. Abnormal blood hepatic protein synthesis in CHF

Blood levels of hepatic proteins are used to evaluate nutritional status, but they are also influenced by many factors other factors. Particularly, the presence of inflammation is known to inversely correlate with circulating levels of hepatic proteins. Indeed, the gene expression of hepatic proteins was decreased associated with local increases in proinflammatory molecules of the liver in this study. However, the mechanism by which inflammation affects hepatic protein is not known [10]. HNF4 regulates the gene expression of transthyretin [16,17]. Although the mechanism by which proinflammatory molecules act on HNF4 expression is unclear, increased levels of SREBPs are known to repress HNF4 gene expression [23].

4.3. Measurement of metabolites using metabolome analysis

The measurement of metabolites in glycolysis and the Krebs cycle provides a snap shot of metabolism. However, based on the findings that ^{18}FDG uptake was increased, the amount of metabolites in glycolysis was increased, the amount of metabolites in the Krebs cycle was decreased, and the TG content was increased, we speculate that acetyl-CoA might be used for *de novo* lipogenesis. Further analysis, in which isotope-labeled glucose or fatty acid is injected and isotope-labeled metabolites are measured, is needed to know how glucose or fatty acids are used to test if the speculation is correct [24,25].

4.4. Potential role of abnormal liver metabolism in cardiac cachexia

Food intake was reduced and blood sugar levels were decreased in this model. During fasting, the liver is expected to deliver energy substrates, such as glucose and FFAs, to peripheral tissues. However, paradoxically, liver incorporated more glucose, the expression of genes related to gluconeogenesis was decreased, the expression of genes related to lipogenesis was increased, and TG content was increased. The response appears to be maladaptive, when the body is

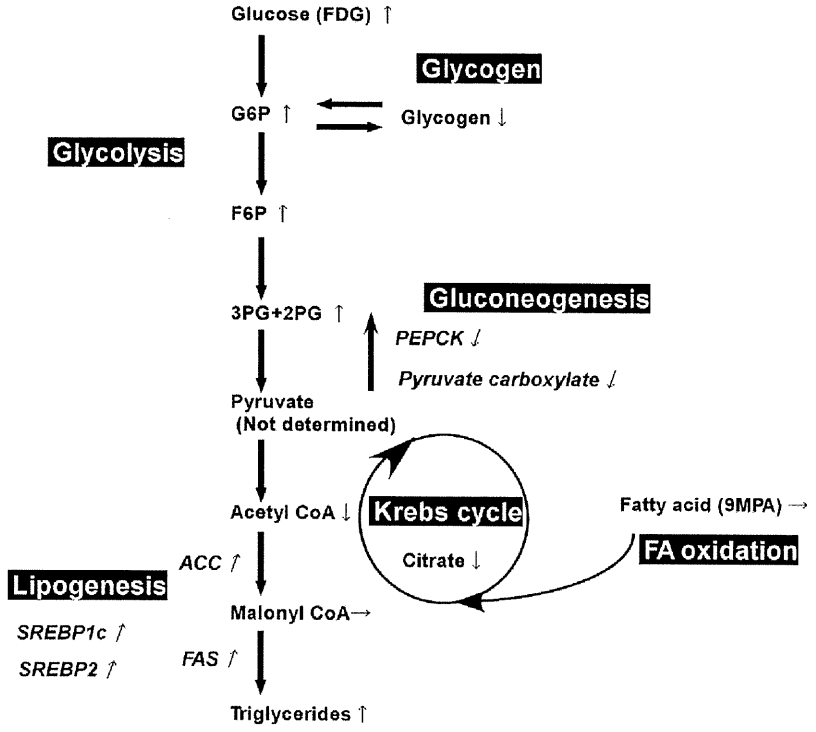

Fig. 10. Summary of the metabolic prolife in liver of CHF rats. Liver incorporated more glucose, gene expression related to gluconeogenesis was decreased, gene expression related to lipogenesis was increased, and TG content was increased in CHF rat liver.

Please cite this article as: Kato T, et al, Analysis of liver metabolism in a rat model of heart failure, Int J Cardiol (2011), doi:10.1016/j.ijcard.2011.07.056

losing weight and peripheral tissues need more substrates to maintain tissue homeostasis. Although this study is an observational one, the findings indicate the abnormal liver metabolism to be a maladaptive process and worsen the CHF. Further study of whether the modulation of liver metabolism ameliorates CHF is needed.

Acknowledgements

The authors of this manuscript have certified that they comply with the Principles of Ethical Publishing in the International Journal of Cardiology [30].

Appendix A. Supplementary data

Supplementary data to this article can be found online at doi:10.1016/j.ijcard.2011.07.056.

References

[1] Neubauer S. The failing heart — an engine out of fuel. N Engl J Med 2007;356:1140–51.
[2] Kato T, Niizuma S, Inuzuka Y, et al. Analysis of metabolic remodeling in compensated left ventricular hypertrophy and heart failure. Circ Heart Fail 2010;3:420–30.
[3] Doehner W, Rauchhaus M, Ponikowski P, et al. Impaired insulin sensitivity as an independent risk factor for mortality in patients with stable chronic heart failure. J Am Coll Cardiol 2005;46:1019–26.
[4] Anker SD, Sharma R. The syndrome of cardiac cachexia. Int J Cardiol 2002;85:51–66.
[5] Simonini A, Long CS, Dudley GA, et al. Heart failure in rats causes changes in skeletal muscle morphology and gene expression that are not explained by reduced activity. Circ Res 1996;79:128–36.
[6] Soga T, Ohashi Y, Ueno Y, Naraoka H, Tomita M, Nishioka T. Quantitative metabolome analysis using capillary electrophoresis mass spectrometry. J Proteome Res 2003;2:488–94.
[7] Rigden DJ, Jellyman AE, Frayn KN, Coppack SW. Human adipose tissue glycogen levels and responses to carbohydrate feeding. Eur J Clin Nutr 1990;44:689–92.
[8] Folch J, Lees M, Stanley GHS. A simple method for the isolation and purification of total lipids from animal tissues. J Biol Chem 1957;226:497–509.
[9] Shioi T, Kang PM, Douglas PS, et al. The conserved phosphoinositide 3-kinase pathway determines heart size in mice. EMBO J 2000;19:2537–48.
[10] Furman MP, Charney P, Mueller CM. Hepatic proteins and nutrition assessment. J Am Diet Assoc 2004;104:1258–64.
[11] Bernstein LH, Ingenbleek Y. Transthyretin: its response to malnutrition and stress injury. Clinical usefulness and economic implications. Clin Chem Lab Med 2002;40:1344–8.
[12] Inoko M, Kihara Y, Morii I, Fujiwara H, Sasayama S. Transition from compensatory hypertrophy to dilated, failing left ventricles in Dahl salt-sensitive rats. Am J Physiol 1994;267:H2471–82.
[13] Carr JG, Stevenson LW, Walden JA, Heber D. Prevalence and haemodynamic correlates of malnutrition in severe congestive heart failure secondary to ischaemic or idiopathic dilated cardiomyopathy. Am J Cardiol 1989;63:709–13.
[14] Shimano H. SREBPs: physiology and pathophysiology of the SREBP family. FEBS J 2009;276:616–21.
[15] Raghow R, Yellaturu C, Deng X, Park EA, Elam MB. SREBPs: the crossroads of physiological and pathological lipid homeostasis. Trends Endocrinol Metab 2008;19:65–73.
[16] Costa RH, Grayson DR. Site-directed mutagenesis of hepatocyte nuclear factor (HNF) binding sites in the mouse transthyretin (TTR) promoter reveal synergistic interactions with its enhancer region. Nucleic Acids Res 1991;19:4139–45.
[17] Wang Z, Burke PA. Hepatocyte nuclear factor-4α interacts with other hepatocyte nuclear factors in regulating transthyretin gene expression. FEBS J 2010;277:4066–75.
[18] Fon Tacer K, Kuzman D, Seliskar M, Pompon D, Rozman D. TNF-alpha interferes with lipid homeostasis and activates acute and proatherogenic processes. Physiol Genomics 2007;31:216–27.
[19] Sharma R, Anker SD. Cytokines, apoptosis and cachexia: the potential for TNF antagonism. Int J Cardiol 2002;85:161–71.
[20] Yndestad A, Damås JK, Oie E, Ueland T, Gullestad L, Aukrust P. Systemic inflammation in heart failure — the whys and wherefores. Heart Fail Rev 2006;11:83–92.
[21] Kleemann R, Verschuren L, van Erk MJ, et al. Atherosclerosis and liver inflammation induced by increased dietary cholesterol intake: a combined transcriptomics and metabolomics analysis. Genome Biol 2007;8:R200.
[22] Aker SD, Belosjorow S, Konietzka I, et al. Serum but not myocardial TNF-alpha concentration is increased in pacing-induced heart failure in rabbits. Am J Physiol Regul Integr Comp Physiol 2003;285:R463–9.
[23] Xie X, Liao H, Dang H, et al. Down-regulation of hepatic HNF4alpha gene expression during hyperinsulinemia via SREBPs. Mol Endocrinol 2009;23:434–43.
[24] Patel AB, de Graaf RA, Mason GF, Rothman DL, Shulman RG, Behar KL. The contribution of GABA to glutamate/glutamine cycling and energy metabolism in the rat cortex in vivo. Proc Natl Acad Sci USA 2005;102:5588–93.
[25] Metallo CM, Walther JL, Stephanopoulos G. Evaluation of ^{13}C isotopic tracers for metabolic flux analysis in mammalian cells. J Biotechnol 2009;144:167–74.
[26] Rodgers JT, Lerin C, Haas W, Gygi SP, Spiegelman BM, Puigserver P. Nutrient control of glucose homeostasis through a complex of PGC-1 and SIRT1. Nature 2005;434:113–8.
[27] Nadler EP, Dickinson EC, Beer-Stolz D, et al. Scavenging nitric oxide reduces hepatocellular injury after endotoxin challenge. Am J Physiol Gastrointest Liver Physiol 2001;281:G173–81.
[28] Puskás LG, Kitajka K, Nyakas C, Barcelo-Coblijn G, Farkas T. Short-term administration of omega 3 fatty acids from fish oil results in increased transthyretin transcription in old rat hippocampus. Proc Natl Acad Sci USA 2003;100:1580–5.
[29] Li J, Tao R, Wu W, et al. Transcriptional profiling and hepatogenic potential of acute hepatic failure-derived bone marrow mesenchymal stem cells. Differentiation 2010;80:166–74.
[30] Shewan LG, Coats AJ. Ethics in the authorship and publishing of scientific articles. Int J Cardiol 2010;144:1–2.

Please cite this article as: Kato T, et al, Analysis of liver metabolism in a rat model of heart failure, Int J Cardiol (2011), doi:10.1016/j.ijcard.2011.07.056

Advance Publication by J-STAGE

Circulation Journal
Official Journal of the Japanese Circulation Society
http://www.j-circ.or.jp

Transition From Asymptomatic Diastolic Dysfunction to Heart Failure With Preserved Ejection Fraction

– Roles of Systolic Function and Ventricular Distensibility –

Yoshihiro Aizawa, MD; Yasushi Sakata, MD; Toshiaki Mano, MD; Yasuharu Takeda, MD; Tomohito Ohtani, MD; Shunsuke Tamaki, MD; Yosuke Omori, MD; Yasumasa Tsukamoto, MD; Atsushi Hirayama, MD; Issei Komuro, MD; Kazuhiro Yamamoto, MD, PhD

Background: Systolic abnormality, as well as diastolic dysfunction, is observed in patients with heart failure with preserved ejection fraction (HFPEF). However, the role of these 2 conditions in the transition from asymptomatic diastolic dysfunction to symptomatic heart failure remains unclear. We recently demonstrated that diastolic wall strain (DWS) inversely correlates to the myocardial stiffness constant.

Methods and Results: This study consisted of 127 subjects: 52 consecutive HFPEF patients (HFPEF group), 50 asymptomatic hypertensive patients with ejection fraction ≥50% whose age, gender and left ventricular (LV) mass index matched those of the HFPEF group (HT group) and 25 normal volunteers (Normal group). The tissue Doppler-derived peak systolic and early diastolic velocities of the mitral annulus were significantly decreased in groups HFPEF and HT than in group Normal, but were not significantly different between groups HFPEF and HT. DWS was significantly lower in group HFPEF than in group HT.

Conclusions: The transition from asymptomatic diastolic dysfunction stage to HFPEF stage is not attributed to progression of systolic abnormality, and exacerbation of LV distensibility rather than relaxation plays a crucial role in the development of HFPEF.

Key Words: Diastole; Heart failure; Systole

In the past 2 decades, the prevalence of heart failure with preserved ejection fraction (HFPEF) has increased, and its prognosis is poor.[1,2] Left ventricular (LV) diastolic dysfunction proven by invasive assessment is present in most patients with HFPEF,[3,4] and has been implicated as a major factor responsible for the clinical syndromes of this phenotype of HF.

Several clinical studies have shown that there is systolic as well as diastolic dysfunction in patients with HFPEF,[5–8] and there has been a suspicion that the systolic dysfunction is responsible for the symptoms of HFPEF patients. However, the previous studies compared HFPEF patients to normal subjects. There are many asymptomatic patients with diastolic dysfunction,[9] and a comparison between patients with asymptomatic diastolic dysfunction and those with HFPEF is desirable to address the issue of the contribution of systolic dysfunction to the symptoms of HFPEF.

LV relaxation and compliance/distensibility are principal components of diastolic function.[10] Our previous experimental study demonstrated that the transition from the compensatory LV hypertrophic stage to HFPEF in the hypertensive heart was associated with an increase in the myocardial stiffness constant and a lack of the further change in the time constant of LV relaxation.[11] To clinically clarify the contribution of diastolic dysfunction to the incidence of HFPEF, LV relaxation and compliance/distensibility should be assessed respectively. Tissue Doppler imaging (TDI) of the mitral annulus level is widely used for noninvasive detection of diastolic dysfunction, but principally reflects LV relaxation.[12] Another noninvasive index of LV diastolic dysfunction is elevation of the LV filling pressure secondary to diastolic dysfunction.[10] Recently, we reported that LV distensibility can be evaluated noninvasively by echocardiography.[13]

The aim of this study was to investigate the contribution of

Received October 11, 2010; revised manuscript received October 29, 2010; accepted November 12, 2010; released online January 27, 2011 Time for primary review: 9 days

Department of Cardiovascular Medicine, Osaka University Graduate School of Medicine, Suita (Y.A., Y.S., T.M., Y. Takeda, T.O., S.T., Y.O., Y. Tsukamoto, I.K., K.Y.); Division of Cardiology, Department of Internal Medicine, Nihon University School of Medicine, Tokyo (Y.A., A.H.); and The Center for Advanced Medical Engineering and Informatics, Osaka University, Suita (S.T., K.Y.), Japan

Mailing address: Kazuhiro Yamamoto, MD, PhD, FACC, Department of Cardiovascular Medicine, Osaka University Graduate School of Medicine, 2-2 Yamadaoka, Suita 565-0871, Japan. E-mail: kazuhiro@medone.med.osaka-u.ac.jp

ISSN-1346-9843 doi:10.1253/circj.CJ-10-1037

Table 1. Definition of Heart Failure

Major	Minor
Paroxysmal nocturnal dyspnea	Edema
Orthopnea	Night cough
Abnormal jugular venous distention	Dyspnea on exertion
Pulmonary rales	Hepatomegaly
Cardiomegaly	Pleural effusion
Pulmonary edema	Tachycardia (>120beats/min)
Presence of a third heart sound	Weight loss≥4.5 kg in 5 days
Central venous pressure>16cmH_2O	(Considered a major criterion if it occurs during therapeutic interventions for heart failure)
Hepatojugular reflux	

A patient is considered to have heart failure if 2 major criteria are present or if 1 major and 2 minor criteria are present concurrently.

Table 2. Clinical Characteristics of All Subjects

	Group Normal	Group HT	Group HFPEF
n	25	50	52
Age (years)	43±17	64±11*	68±12*
Men (%)	56	58	50
Height (m)	1.65±0.10	1.59±0.10*	1.59±0.09*
Weight (kg)	61±11	60±12	60±16
Body mass index (kg/m^2)	22±3.3	23±3.1	24±4.9
Comorbidity			
HT (%)		100	65†
Diabetes mellitus (%)		20	26
Dyslipidemia (%)		30	33
Medication			
Diuretic (%)		28	55†
Calcium-channel blocker (%)		54	53
β-blocker (%)		26	41
Angiotensin-converting enzyme inhibitor (%)		16	20
Angiotensin receptor blocker (%)		68	55
Mineralocorticoid receptor blocker (%)		8	24†
Statin (%)		28	25
Heart rate (beats/min)	66±10	63±8	64±11
Systolic blood pressure (mmHg)	118±11	136±19*	135±22*
Diastolic blood pressure (mmHg)	69±9	72±9	69±14

Values are mean±SD. *P<0.05 vs. Normal group, †P<0.05 vs. HT group.
HT, hypertension; HFPEF, heart failure with preserved ejection fraction.

LV systolic and diastolic dysfunction to the transition from asymptomatic stage to HFPEF.

Methods

Study Subjects

This study consisted of 127 subjects in 3 groups. Of consecutive subjects who underwent echocardiography in Osaka University Hospital between July 2006 and December 2008, 52 outpatients with HFPEF who met the following criteria were selected (HFPEF group): (1) echocardiographic confirmation of EF≥50%, (2) without known coronary artery disease, segmental wall motion abnormalities, congenital heart disease, severe valve disease, atrial fibrillation, pulmonary disease, active collagen disease or renal failure (serum creatinine concentration >2.5mg/dl), (3) meeting modified Framingham criteria,[14] as previously described[15] (**Table 1**) and (4) clinically stable. Medical records were reviewed by cardiologists to assess each patient's characteristics.

Of consecutive subjects who underwent echocardiography in Osaka University Hospital between December 2007 and August 2008, we selected 50 asymptomatic outpatients with hypertension and EF≥50% whose age, gender and LV mass index matched with those of HFPEF group (HT group). Patients with known coronary artery disease, segmental wall motion abnormalities, congenital heart disease, severe valve disease, atrial fibrillation, pulmonary disease, active collagen disease or renal failure were excluded. We also included 25 consecutive normal volunteers without cardiac disease, hypertension, dyslipidemia or diabetes mellitus (Normal group).

This retrospective study was approved by the Osaka University Hospital Ethics Committee. The original data for the patients in the HFPEF and HT groups were obtained from clinical practice and were retrospectively analyzed. Thus, in

Table 3. Echocardiographic Data

	Group Normal	Group HT	Group HFPEF
LV ejection fraction (%)	66±7	67±6	64±8
Left atrial dimension (mm)	33±5	39±6*	43±7*,†
LV end-diastolic dimension (mm)	48±5	48±6	48±6
LV end-systolic dimension (mm)	30±3	30±4	31±6
Interventricular septal thickness at end-diastole (mm)	7±1	10±2*	11±3*
Interventricular septal thickness at end-systole (mm)	10±1	13±2*	13±3*
LV posterior wall thickness at end-diastole (mm)	7±1	9±1	9±2
LV posterior wall thickness at end-systole (mm)	13±2	15±2*	14±3†
LV mass index (g/m^2)	70±16	102±26*	105±42*
LV relative wall thickness	0.32±0.05	0.39±0.07*	0.39±0.09*
Tricuspid regurgitation peak gradient (mmHg)	15±3	21±5*	26±14*,†
Mitral E (cm/s)	70±19	63±15	66±21
Mitral A (cm/s)	52±16	75±14*	77±27*
Mitral E/A ratio	1.5±0.5	0.9±0.2*	1.0±0.6*
Deceleration time of E wave (ms)	182±32	205±40	221±65*
Isovolumic relaxation time (ms)	67±14	72±17	77±25
E' (cm/s)	9.6±2.6	5.9±1.5*	5.5±1.7*
A' (cm/s)	8.7±1.7	9.1±1.7	8.3±2.1†
E/E' ratio	6.6±1.4	9.0±2.4*	11.9±4.5*,†

Values are mean±SD, *P<0.05 vs. Normal group, †P<0.05 vs. HT group.
LV, left ventricular; E/A, ratio of peak mitral E wave velocity to peak mitral A wave velocity; A', peak late diastolic myocardial velocity at septal position recorded by tissue Doppler imaging; E/E', ratio of peak mitral E wave velocity to peak early diastolic myocardial velocity at septal position recorded by tissue Doppler imaging. Other abbreviations see in Table 2.

compliance with the guiding principles of the Ministry of Health, Labour and Welfare, Japan, with regard to epidemiological study, the Ethics Committee approved data collection without the written informed consent of each patient. The normal volunteers gave written informed consent.

Data Collection

Echocardiographic recordings were obtained in all patients using commercially available machines and EF, relative wall thickness and LV mass were calculated as previously described.[13,16,17] EF was calculated by a modification of the method of Quinones et al.[18] The LV mass index was calculated as a ratio of LV mass to body surface area.[13,16] The right ventricular to right atrial pressure gradient during systole (tricuspid regurgitation peak gradient) was approximated by the modified Bernoulli equation as $4v^2$, where v is the velocity of the tricuspid regurgitation jet in m/s. Transmitral flow velocity curves were recorded to measure peak early diastolic (E) and late diastolic (A) velocities.[16] TDI of the mitral annulus level was obtained at the septal position in order to measure the early diastolic (E'), late diastolic (A') and systolic (S') myocardial velocities as previously described.[13,17] Systolic function was assessed with S',[19–21] and LV relaxation was assessed with E'.[12] From our recent study, we reported that diastolic wall strain (DWS defined as follows) theoretically reflects LV distensibility according to linear elastic theory and was significantly and inversely correlated with myocardial stiffness constant in an animal HFPEF model.[13] Thus, we used DWS as an index of LV distensibility.

DWS=(LV posterior wall thickness at end-systole−LV posterior wall thickness at end-diastole)/LV posterior wall thickness at end-systole.

Statistical Analysis

Results are expressed as mean±SD. All statistical analyses were performed using commercially available statistical software (STATVIEW version 5.0, SAS Institute Inc, Cary, NC, USA). Differences between 2 groups were assessed using Student's t-test. Comparisons of nonparametric data were performed by chi-square test. Differences among 3 groups were assessed using 1-way analysis of variance followed by Fisher's protected least significant difference test. Correlations of 2 indices were assessed using linear regression analysis with the least-square method. P<0.05 was considered statistically significant.

Results

The characteristics of the study subjects are summarized in **Table 2**. Age and systolic blood pressure were higher in the HT and HFPEF groups than in the Normal group, and did not differ between the 2 groups. The prevalence of hypertension was less in the HFPEF group than in the HT group, but that of diabetes mellitus or dyslipidemia was not different between the 2 groups. Diuretic and mineralocorticoid receptor blocker were prescribed in more patients of the HFPEF group than of the HT group.

Echocardiographic data are summarized in **Table 3**. There was no difference in LV end-diastolic dimension or EF among the 3 groups. The E/A ratio and E' were lower, and the LV mass index and relative wall thickness were higher in the HT and HFPEF groups than in the Normal group. These indices did not differ between the HT and HFPEF groups. Left atrial dimension, tricuspid regurgitation peak gradient and E/E' ratio were the highest in the HFPEF group and the lowest in the Normal group.

S' was significantly lower in the HFPEF and HT groups

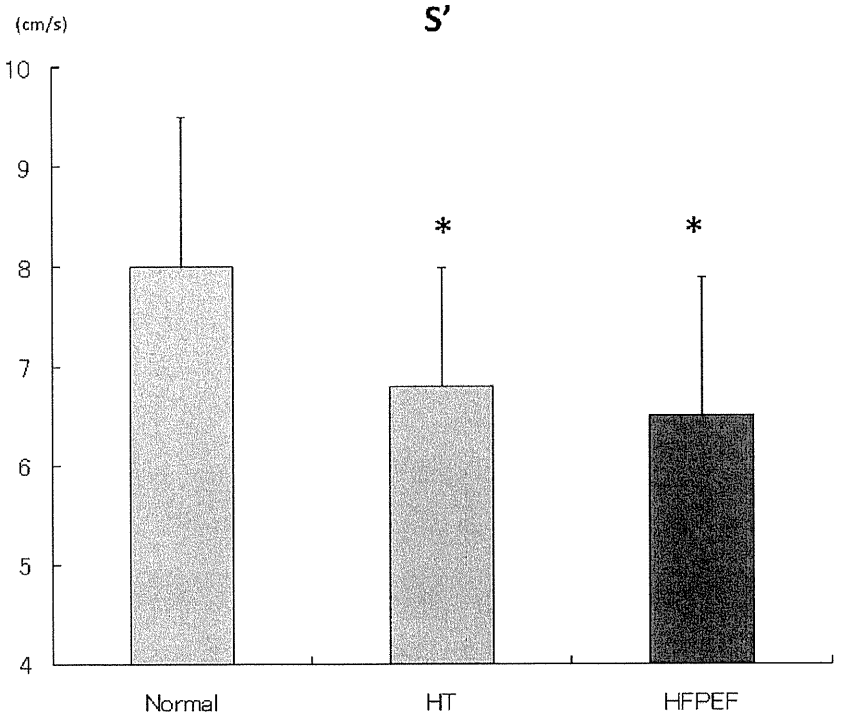

Figure 1. Comparison of S' among the Normal, HT and HFPEF groups. *P<0.05 vs. Normal group. S', peak systolic myocardial velocity at septal position recorded by tissue Doppler imaging. HFPEF, heart failure with preserved ejection fraction; HT, hypertension.

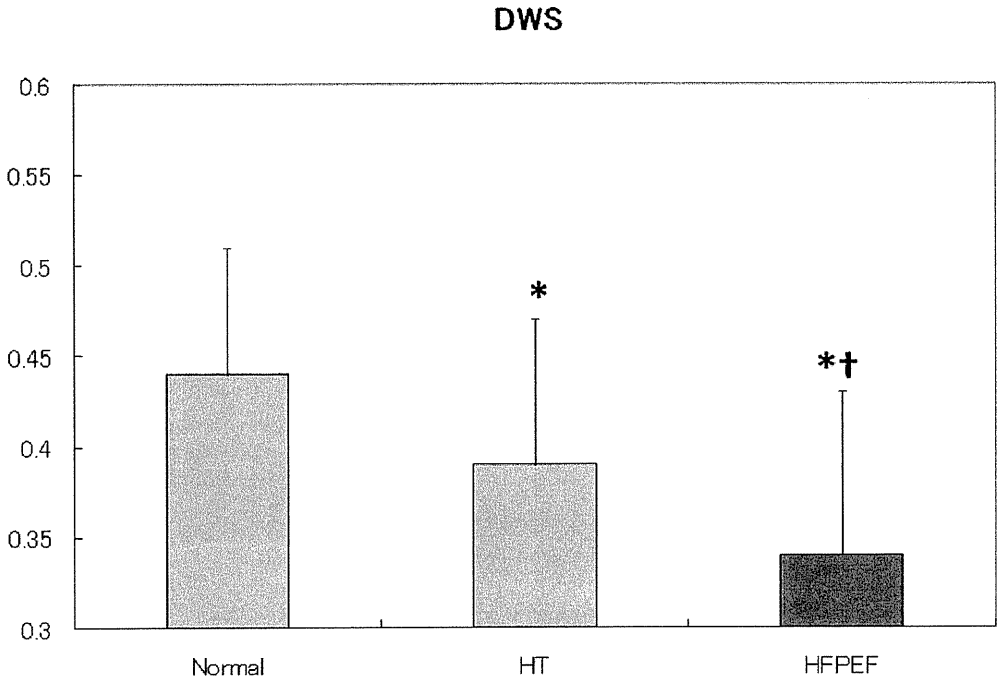

Figure 2. Comparison of diastolic wall strain (DWS) among the Normal, HT and HFPEF groups. *P<0.05 vs. Normal group. †P<0.05 vs. HT group. HFPEF, heart failure with preserved ejection fraction; HT, hypertension.

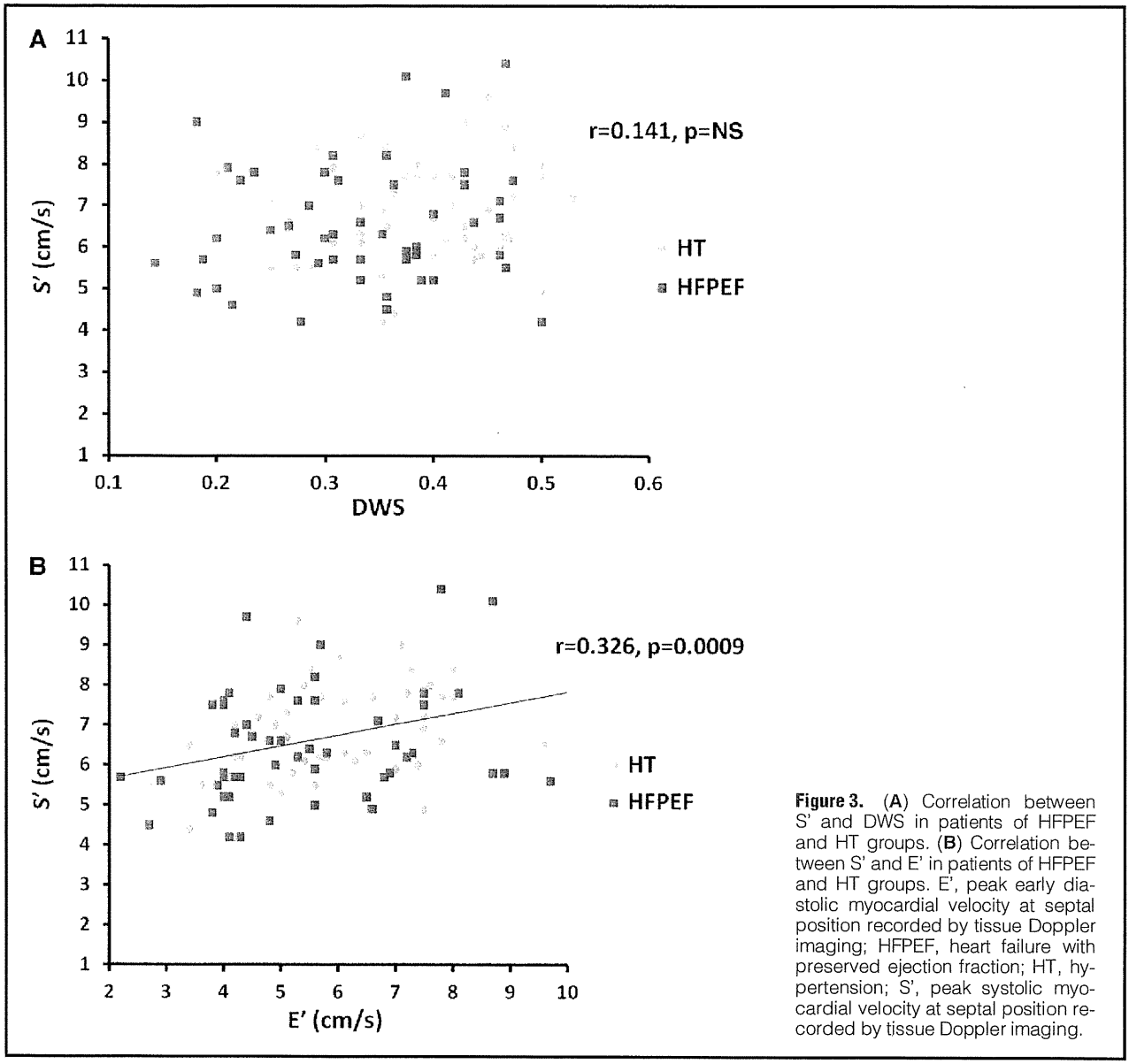

Figure 3. (**A**) Correlation between S' and DWS in patients of HFPEF and HT groups. (**B**) Correlation between S' and E' in patients of HFPEF and HT groups. E', peak early diastolic myocardial velocity at septal position recorded by tissue Doppler imaging; HFPEF, heart failure with preserved ejection fraction; HT, hypertension; S', peak systolic myocardial velocity at septal position recorded by tissue Doppler imaging.

than in the Normal group, and was not significantly different between the HT and HEPEF groups (**Figure 1**). DWS was lowest in the HFPEF group and highest in the Normal group (**Figure 2**). There was no significant correlation between S' and DWS in the patients of the HFPEF and HT groups (**Figure 3A**). In contrast, S' significantly correlated with E' (**Figure 3B**).

The same analysis was conducted only in patients without elevated LV filling pressures (ie, patients with E/E' ratio <15).[22] DWS was significantly lower in the HFPEF group (n=43) than in the HT group (n=48) (0.33±0.09 vs. 0.39±0.07, P<0.05). S' did not differ between the 2 groups.

Discussion

The results of the current study showed that LV longitudinal systolic function and LV relaxation were impaired to the same degree in the HT and HFPEF groups, but that LV distensibility, as assessed by DWS, was further exacerbated in the HFPEF group compared to the HT group.

Our animal experimental study showed that the impairment of LV compliance/distensibility progresses, but LV relaxation abnormality does not, in the transition from asymptomatic LV diastolic dysfunction to the HFPEF stage in a hypertensive HFPEF model.[11] The currently available noninvasive indices for LV diastolic function represent LV relaxation (E' or flow propagation velocity of early diastolic flow)[12,23] or LV filling pressure (E/E'),[22] and it has been difficult to noninvasively assess LV compliance or distensibility. We recently demonstrated that DWS inversely correlates with the myocardial stiffness constant and is not affected by preload alteration.[13] The current study showed that DWS was lower in HFPEF patients than in asymptomatic hypertensive patients, despite similar decreases in S' and E'. The same results were obtained even when excluding patients with elevated LV filling pressure. Thus, the significant difference in DWS between the HFPEF and HT groups cannot be explained by the high prevalence of patients with an elevated

LV filling pressure in the HFPEF group compared to the HT group, and progressive exacerbation of LV distensibility may play a crucial role in the development of HFPEF. Melenovsky et al reported that LV hypertrophy and left atrial dilatation, not low S', were cardiovascular features that discriminated patients with HFPEF from those with asymptomatic LV hypertrophy.[24] In this study, the left atrial dimension was greater in the HFPEF group than in the HT group, but the LV mass index was not different between the 2 groups. Left atrial enlargement indicates LV diastolic dysfunction,[25] but also reflects abnormality of both LV relaxation and distensibility. Vinereanu et al showed a significant correlation of S' with the indices of LV relaxation and filling pressure, and concluded that diastolic function was impaired in parallel with systolic function.[26] The significant correlation between the indices for systolic function and relaxation was also observed in our study, as indicated by the correlation between S' and E' (**Figure 3B**). Vinereanu et al did not assess LV distensibility, and we demonstrated a lack of correlation between S' and DWS (**Figure 3A**). The results of the present study suggest that the development of HFPEF from the asymptomatic stage is associated with progressive LV diastolic dysfunction, which is primarily due to exacerbation of LV distensibility. In addition, we demonstrated that diastolic function is not impaired in parallel with systolic function if LV distensibility is evaluated in the assessment of diastolic function. Our recent preliminary study demonstrated that HFPEF patients with low DWS have a poor prognosis.[27] Thus, LV distensibility is likely to play a crucial role in the pathogenesis of this type of HF.

Several previous studies have reported that S', the most sensitive marker of systolic function,[19–21] was reduced in patients with HFPEF,[5–8] and have argued that HFPEF is caused by systolic dysfunction. However, those previous studies compared HFPEF patients to normal subjects. Redfield et al showed that there are many asymptomatic patients with diastolic dysfunction,[9] indicating that there is a stage of asymptomatic diastolic dysfunction between the normal and HFPEF stages. We found that the S' of HFPEF patients was decreased as compared to normal subjects, which is compatible with the findings of previous studies;[5–8] however, we also demonstrated that S' did not differ between asymptomatic hypertensive patients and HFPEF patients. These observations are partly supported by the data from other studies.[24,26] Thus, the progression of systolic dysfunction may not be the principal cause for the transition from asymptomatic diastolic dysfunction to HFPEF. Yu et al reported that S' was lower in patients with HFPEF than in those with asymptomatic diastolic dysfunction, and suggested the contribution of progressive systolic dysfunction to HFPEF.[28] However, E' was also significantly lower in patients with HFPEF than in those with asymptomatic diastolic dysfunction, and LV distensibility was not assessed in their study. In our study, E' was similarly decreased in the HFPEF and HT groups (**Table 2**). Thus, the diastolic function of patients with asymptomatic diastolic dysfunction may have been impaired to a lesser degree in Yu's study than in our study, which would explain the different conclusions.

Study Limitations

First, this hospital-based study provided cross-sectional observations only and cannot adequately prove causality. Second, it was a retrospective study, and medications were not withheld for echocardiographic examination of patients of the HT and HFPEF groups. Third, the number of study subjects was not large. Fourth, brain natriuretic peptide levels were not measured, and it is unclear how many patients met the criteria of HFPEF proposed by the European Society of Cardiology.[29] Fifth, all the study subjects were Japanese. A number of demographic parameters may affect the cardiovascular abnormalities and comorbidities in HFPEF patients, and the current results may not be able to be simply extrapolated to other races. Sixth, the Normal group was not matched by age with the HT and HFPEF groups. The difference in some parameters between the Normal and HT groups may be partly explained by aging rather than hypertension. However, there was no difference in age between the HT and HFPEF groups, and our conclusion about the factors that are related to the transition from the asymptomatic stage with diastolic dysfunction to the HFPEF stage may not be affected by the difference in age between the Normal group and the HT or HFPEF group.

Conclusions

The current study results suggest that the transition from the asymptomatic stage with diastolic dysfunction to the HFPEF stage can not be attributed to progression of systolic abnormality, and that exacerbation of LV distensibility plays a crucial role in the development of HFPEF.

Acknowledgments

The authors are grateful to Ms Keiko Katsuki and Ms Yumiko Kobayashi for their technical assistance. Shunsuke Tamaki, MD is a research assistance of the Global COE Program.

Disclosures

Conflict of Interest: None declared.

Funding Sources: This study was supported in part by grants from the Japanese Society for the Promotion of Science.

References

1. Owan TE, Hodge DO, Herges RM, Jacobsen SJ, Roger VL, Redfield MM. Trends in prevalence and outcome of heart failure with preserved ejection fraction. *N Engl J Med* 2006; **355:** 251–259.
2. Miyagishima K, Hiramitsu S, Kimura H, Mori K, Ueda T, Kato S, et al. Long term prognosis of chronic heart failure: Reduced vs preserved left ventricular ejection fraction. *Circ J* 2009; **73:** 92–99.
3. Zile MR, Baicu CF, Gaasch WH. Diastolic heart failure: Abnormalities in active relaxation and passive stiffness of the left ventricle. *N Engl J Med* 2004; **350:** 1953–1959.
4. Penicka M, Bartunek J, Trakalova H, Hrabakova H, Maruskova M, Karasek J, et al. Heart failure with preserved ejection fraction in outpatients with unexplained dyspnea: A pressure-volume loop analysis. *J Am Coll Cardiol* 2010; **55:** 1701–1710.
5. Yip G, Wang M, Zhang Y, Fung JW, Ho PY, Sanderson JE. Left ventricular long axis function in diastolic heart failure is reduced in both diastole and systole: Time for a redefinition? *Heart* 2002; **87:** 121–125.
6. Nikitin NP, Witte KK, Clark AL, Cleland JG. Color tissue Doppler-derived long-axis left ventricular function in heart failure with preserved global systolic function. *Am J Cardiol* 2002; **90:** 1174–1177.
7. Petrie MC, Caruana L, Berry C, McMurray JJ. "Diastolic heart failure" or heart failure caused by subtle left ventricular systolic dysfunction? *Heart* 2002; **87:** 29–31.
8. Bruch C, Gradaus R, Gunia S, Breithardt G, Wichter T. Doppler tissue analysis of mitral annular velocities: Evidence for systolic abnormalities in patients with diastolic heart failure. *J Am Soc Echocardiogr* 2003; **16:** 1031–1036.
9. Redfield MM, Jacobsen SJ, Burnett JC Jr, Mahoney DW, Bailey KR, Rodeheffer RJ. Burden of systolic and diastolic ventricular dysfunction in the community: Appreciating the scope of the heart failure epidemic. *JAMA* 2003; **289:** 194–202.
10. Yamamoto K, Sakata Y, Ohtani T, Takeda Y, Mano T. Heart failure with preserved ejection fraction. *Circ J* 2009; **73:** 404–410.
11. Masuyama T, Yamamoto K, Sakata Y, Doi R, Nishikawa N,

Kondo H, et al. Evolving changes in Doppler mitral flow velocity pattern in rats with hypertensive hypertrophy. *J Am Coll Cardiol* 2000; **36:** 2333–2338.
12. Nagueh SF, Sun H, Kopelen HA, Middleton KJ, Khoury DS. Hemodynamic determinants of the mitral annulus diastolic velocities by tissue Doppler. *J Am Coll Cardiol* 2001; **37:** 278–285.
13. Takeda Y, Sakata Y, Higashimori M, Mano T, Nishio M, Ohtani T, et al. Noninvasive assessment of wall distensibility with the evaluation of diastolic epicardial movement. *J Card Fail* 2009; **15:** 68–77.
14. McKee PA, Castelli WP, McNamara PM, Kannel WB. The natural history of congestive heart failure: The Framingham study. *N Engl J Med* 1971; **285:** 1441–1446.
15. The J-DHF Program Committee. Rationale and design of a randomized trial to assess the effects of beta-blocker in diastolic heart failure; Japanese Diastolic Heart Failure Study (J-DHF). *J Card Fail* 2005; **11:** 542–547.
16. Yamaguchi H, Yoshida J, Yamamoto K, Sakata Y, Mano T, Akehi N, et al. Elevation of plasma brain natriuretic peptide is a hallmark of diastolic heart failure independent of ventricular hypertrophy. *J Am Coll Cardiol* 2004; **43:** 55–60.
17. Takeda Y, Sakata Y, Mano T, Nishio M, Ohtani T, Hori M, et al. Noninvasive assessment of diastolic function in subjects with preserved left ventricular ejection fraction: Usefulness of color kinetic imaging. *J Card Fail* 2008; **14:** 569–576.
18. Quinones MA, Waggoner AD, Reduto LA, Nelson JG, Young JB, Winters WL Jr, et al. A new, simplified and accurate method for determining ejection fraction with two-dimensional echocardiography. *Circulation* 1981; **64:** 744–753.
19. Takeda S, Rimington H, Smeeton N, Chambers J. Long axis excursion in aortic stenosis. *Heart* 2001; **86:** 52–56.
20. Vinereanu D, Ionescu AA, Fraser AG. Assessment of left ventricular long axis contraction can detect early myocardial dysfunction in asymptomatic patients with severe aortic regurgitation. *Heart* 2001; **85:** 30–36.
21. Vinereanu D, Florescu N, Sculthorpe N, Tweddel AC, Stephens MR, Fraser AG. Differentiation between pathologic and physiologic left ventricular hypertrophy by tissue Doppler assessment of long-axis function in patients with hypertrophic cardiomyopathy or systemic hypertension and in athletes. *Am J Cardiol* 2001; **88:** 53–58.
22. Ommen SR, Nishimura RA, Appleton CP, Miller FA, Oh JK, Redfield MM, et al. Clinical utility of Doppler echocardiography and tissue Doppler imaging in the estimation of left ventricular filling pressures: A comparative simultaneous Doppler-catheterization study. *Circulation* 2000; **102:** 1788–1794.
23. Takatsuji H, Mikami T, Urasawa K, Teranishi J, Onozuka H, Takagi C, et al. A new approach for evaluation of left ventricular diastolic function: Spatial and temporal analysis of left ventricular filling flow propagation by color M-mode Doppler echocardiography. *J Am Coll Cardiol* 1996; **27:** 365–371.
24. Melenovsky V, Borlaug BA, Rosen B, Hay I, Ferruci L, Morell CH, et al. Cardiovascular features of heart failure with preserved ejection fraction versus nonfailing hypertensive left ventricular hypertrophy in the urban Baltimore community: The role of atrial remodeling/dysfunction. *J Am Coll Cardiol* 2007; **49:** 198–207.
25. Pritchett AM, Mahoney DW, Jacobsen SJ, Rodeheffer RJ, Karon BL, Redfield MM. Diastolic dysfunction and left atrial volume: A population-based study. *J Am Coll Cardiol* 2005; **45:** 87–92.
26. Vinereanu D, Nicolaides E, Tweddel AC, Fraser AG. "Pure" diastolic dysfunction is associated with long-axis systolic dysfunction: Implications for the diagnosis and classification of heart failure. *Eur J Heart Fail* 2005; **7:** 820–828.
27. Ohtani T, Yamamoto K, Dunlay SM, Weston SA, Roger VL, Redfield MM. Severity of LV diastolic stiffness as assessed by the diastolic wall strain index is associated with worse outcomes in heart failure with preserved ejection fraction (abstract). *Circulation* 2010; **122**(21 Suppl): A12731.
28. Yu CM, Lin H, Yang H, Kong SL, Zhang Q, Lee SW. Progression of systolic abnormalities in patients with "isolated" diastolic heart failure and diastolic dysfunction. *Circulation* 2002; **105:** 1195–1201.
29. Paulus WJ, Tschope C, Sanderson JE, Rusconi C, Flachskampf FA, Rademakers FE, et al. How to diagnose diastolic heart failure: A consensus statement on the diagnosis of heart failure with normal left ventricular ejection fraction by the Heart Failure and Echocardiography Associations of the European Society of Cardiology. *Eur Heart J* 2007; **28:** 2539–2550.

特集2「移植医療の新展開—改正臓器移植法施行後1年を経過して—」

改正臓器移植法下における心臓移植実施の現状と問題点

中谷武嗣，戸田宏一，簗瀬正伸，藤田知之，小林順二郎，瀬口　理，
村田欣洋，佐藤琢真，角南春樹，堀　由美子，長岡紀江，和田恭一，
植田初江，宮田茂樹，内藤博昭
国立循環器病研究センター

はじめに

臓器移植法施行によりわが国においても心臓移植が実施されるようになり，1999年から開始された。施行数は徐々に増加し，2006年以降年間10例施行されるようになった（**図1**）[1]。しかし，心臓移植待機者も増加し，待機時間も延長するようになった。2009年に改正臓器移植法が制定され，2010年7月から施行されたが，改正臓器移植法が施行される2010年6月までの心臓移植実施数79例に対し，施行後2011年9月10日までの施行数は41例と著明な増加を認めている（**図1**）。国立循環器病研究センターにおいては，1999年5月に第1例目を施行してから，これまでに39例の心臓移植を実施してきた。年次別の施行数を**図2**に示すが，改正臓器移植法実施までは27例で年に数例であった。しかし，改正臓器移植実施後は1年3カ月の間に12例施行するようになった。このような心臓移植の現状と問題点について，当センターにおけるこれまでの経過を踏まえ報告する。

図1　わが国における心臓移植の年次推移

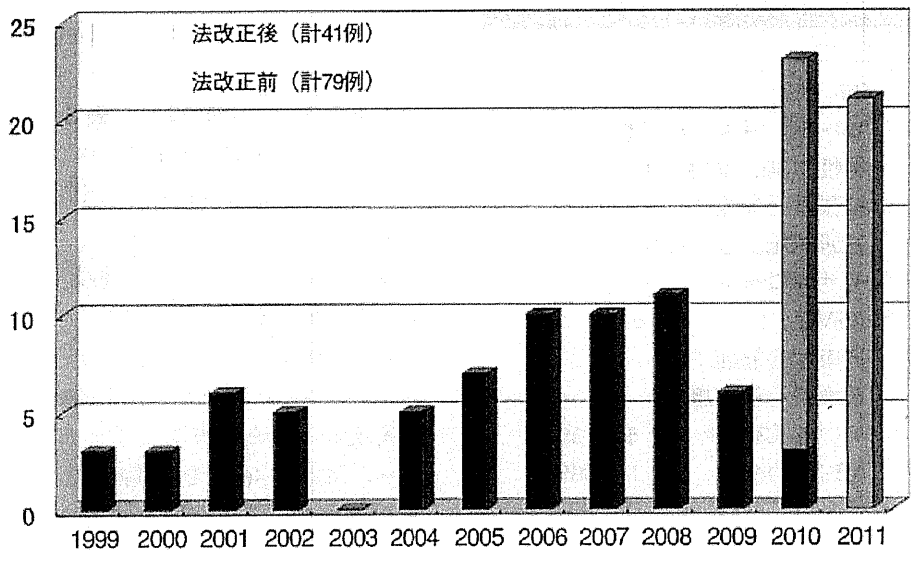

図2　NCVCにおける心臓移植施行数の年次推移

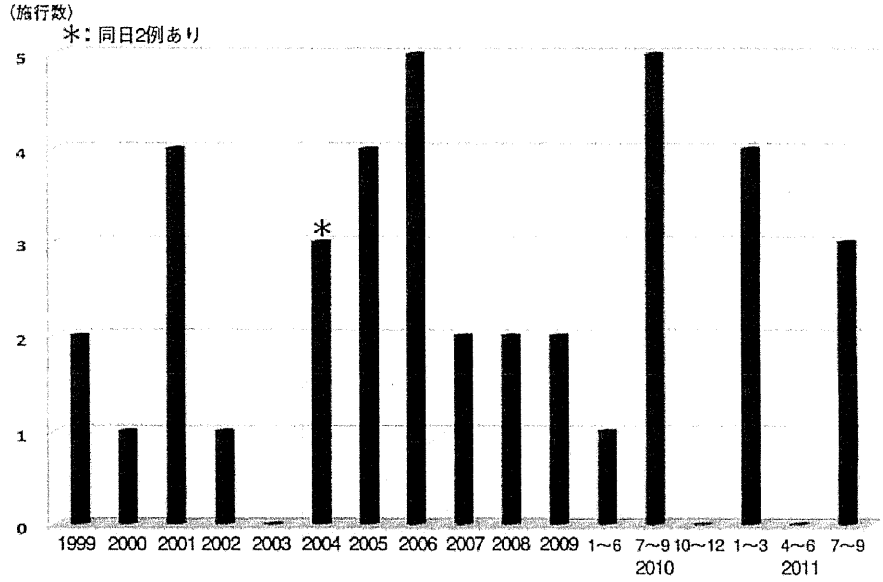

国立循環器病研究センターにおける心臓移植例

1999年5月から2011年9月までに，当センターにおいて39例の心臓移植を実施してきた（表1）。移植時年齢は平均38歳で，60歳以上が2例含まれるが，ともに，体外設置型左心補助人工心臓（LVAS）装着にて3年以上補助を行っていた症例であった。原病は82%が拡張型心筋症で，うち1例は右胸心を伴っていた。待機状況は全例Status 1で，87%は各種LVASによるブリッジ例であった（表2）。用いたLVASは，85%が体外設置型のNipro（Toyobo）製で，15%は拍動流および連続流ポンプによる植込型であった。待機期間は，平均982日間で，Status 1での待機期間は平均818日，最長1,476日に及んだ。また，LVAS補助期間は，平均882日で，最長はNipro（Toyobo）製体外設置型による1,730日に及んだ。39例中最近施行した2例は入院加療中であるが，他の37例は退院した。

表1　国立循環器病研究センターにおける心臓移植(1)

症例数	39
移植時年齢	14～61（平均38）歳
性別	男性：30，女性：9
原病	拡張型心筋症：32*
	拡張相肥大型心筋症：1
	心サルコイドーシス：2
	ARVC：1
	拘束型心筋症：2
	虚血性心筋疾患：1
血液型	A：15（38%），B：5（13%）
	AB：4（11%），O：14（38%）

*：右胸心1例含む

施行数の推移をみると，同時に心臓移植を施行したこともあるが，臓器移植法が改正されるまでは年間5例以内であった（図2）。しかし，改正臓器移植法施行後は2カ月で5例の施行や，4週連続して施行となった。当センターでは，2004年2月に2例同時にドナー情報があり，ともにLVAS装着にて長期待機中の症例であり，2つのドナーチームおよび2つのレシピエントチームを結成し，表3に示すように対応した。2例とも経過は良好で，移植後5日目に移植病棟に転棟し，移植後50日目に退院した。改正臓器移植法施行後，ドナー情報は増加しており，このような同時移植とはならないまでも連続して施行しうる体制であることが必要となっている。

ドナー情報に対しては，ドナー心の状況，搬送，レシピエントの状況などを総合的に考慮して，心臓移植を実施するかを判断することが重要である。当センターにおける36例での検討では，表4に示すように29例がマージナルドナーであった。しかし，表5に示すように，マージナルドナー（29例）と非マージ